Polymer Chemistry

ROYAL SOCIETY OF CHEMISTRY

REVIEW

View Article Online
View Journal | View Issue

Cite this: *Polym. Chem.*, 2025, **16**, 3187

Developments in polytellurophenes and tellurophene-containing polymers: from synthesis to applications

Ailsa K. Edward, [a] Kimia Hosseini, [a] Kristen L. Perry[a] and Dwight S. Seferos *[a,b]

Received 30th April 2025,
Accepted 23rd June 2025

DOI: 10.1039/d5py00439j

rsc.li/polymers

Tellurium is a metalloid, and as such its properties are uniquely placed at the interface between organic and inorganic chemistry. Its five-membered heterocycle, tellurophene, has unique redox, optical, and electronic properties. When integrated as a homopolymer or as a copolymer, tellurophene polymers exhibit novel properties which can be tailored to optimise optoelectronic performance. In this review, we first discuss the inherent properties of the polymers, we then discuss various synthetic methods for their preparation. In addition, we discuss applications of tellurophene polymers in optoelectronic and biomedical applications. Finally, we give an insight into the major challenges still to be overcome for these materials and the future areas for development.

1. Introduction

Some of the most widely used synthetic polymers, including polystyrenes, polytetrafluoroethylenes (PTFE), polyvinyl chlorides (PVC), and polyesters, all contain repeating non-conjugated units and are electrically insulating. In contrast, conjugated polymers are a class of semiconducting materials with extended π-systems formed through a continuous backbone of alternating single and double bonds.[1] This unique configuration along the polymer chains can facilitate mobile delocalised charge carriers as well as charge-transfer from chain to chain, giving rise to exciting optical and electronic applications.[2,3] Recent examples of these include biosignal amplification,[4] electrochromic displays,[5] flexible printed polymer light-emitting diodes (FPPLED),[6] and wearable flexible electronics.[7] The notable conductive nature of these polymers was recognised in 2000 by the Nobel prize in chemistry

[a]*Department of Chemistry, University of Toronto, Lash Miller Chemical Laboratories, Toronto, Ontario M5S 3H6, Canada. E-mail: dwight.seferos@utoronto.ca*
[b]*Department of Chemical Engineering and Applied Chemistry, University of Toronto, 200 College Street, Toronto, Ontario, M5S 3E5, Canada*

Ailsa K. Edward

Ailsa Edward grew up in Dundee, Scotland. She received her PhD in chemistry from the University of St Andrews in 2024, working on the surface functionalisation of metal–organic framework nanoparticles under the co-supervision of Prof. Russell Morris and Dr Euan Kay. Currently, Ailsa is working as a Postdoctoral Fellow in the Seferos group at the University of Toronto. Her research projects involve the automation of chemical processes, specifically targeting polymer post-synthetic modifications, and metal–organic framework syntheses/functionalisation towards CO_2 capture. Outside of the lab, Ailsa enjoys baking, finding nice coffee spots, and attending spin classes.

Kimia Hosseini

Kimia Hosseini received her BSc from the University of British Columbia in 2022. During her undergraduate studies, she worked with Dr Mehrkhodavandi and Dr Schafer on mechanistic investigations for indium and zirconium catalyzed reactions respectively. Currently, Kimia is a PhD student in the Seferos group at the University of Toronto. Her main research interests focus on developing organic cathode materials for use in batteries. Outside of chemistry, she enjoys trying new recipes, going to the gym, and hiking.

to Heeger, MacDiarmid, and Shirakawa for their "discovery and development of conductive polymers".[8] Since this point, the development of novel conjugated polymers has been enhanced significantly by advances in synthetic organic chemistry[9–14] and, more recently, the use of artificial intelligence (AI) and machine learning (ML) strategies to explore and screen new potential conjugated polymers.[15]

Within this material class, inorganic–organic polymers constructed from Group 16 heterocyclic monomers have received significant attention. These include polyfurans, polythiophenes (PThs), polyselenophenes (PSes), and polytellurophenes (PTes). A number of reviews have focused on polyfurans,[16] PThs,[17] and PSes[18,19] as well as Group 16 conjugated polymers in general.[20] Here, we focus specifically on the state-of-the-art synthesis and applications of PTes (polymers built exclusively from tellurophene-based units) and tellurophene-containing polymers (polymers that contain at least one tellurophene-based unit). While earlier examples of PTes have been reviewed by us,[21,22] and more general types of tellurium-containing polymers have been reviewed by others,[23,24] here we briefly discuss the origin of PTes and their tellurophene precursors, including a summary of their properties. We then focus on progress in their synthesis and how their diverse properties can be utilised across optoelectronics and biomedical applications. Included in these examples will be cases where tellurophenes are copolymerised with other chalcogenophenes. Finally, we conclude the review with a perspective for the future of these diverse polymers.

2. Properties of polytellurophenes

2.1. Tellurium

Tellurium (Fig. 1a) is a member of the chalcogens and was initially discovered in 1782.[25,26] Tellurium is a low abundant element and is often sourced as a by-product from the refining of gold, silver and copper. Multiple oxidation states of tellurium exist from −II to +VI and it is a hypervalent element with the largest radius, polarity and lowest electronegativity compared to its related chalcogens (O, S and Se). Tellurium is considered as a metalloid with properties between metals and nonmetals, and applications across organic, inorganic and materials chemistry.[25] Semi-conducting metal tellurides can be found in solar panels, cooling devices and as biomarkers.[25] For example, cadmium telluride (CdTe) solar cells,[27] and tellurium-based tetradymites (M_2X_3, M = group V metal and X = Te) as thermoelectrics, which can operate at room temperature.[28]

Elemental tellurium is also used in alloys,[29] and most notably in electronics. For example, pure tellurium has been employed as a single-element electrical switch with a large drive current density.[30]

2.2. Tellurophene

Tellurophene (Fig. 1b) is a five-membered tellurium-containing heterocycle. Characteristic properties of materials prepared from tellurophene include: strong Te–Te interactions; red-shifted adsorptions; narrow HOMO–LUMO gaps (HOMO = highest occupied molecular orbital, LUMO = lowest occupied molecular orbital); increased Te–C bond length; high polarizability; and high dielectric constants.[22,31] Tellurophene has a relatively lower aromatic character compared to other chalcogenophenes in the order of thiophene > selenophene > tellurophene > furan.[32] The tellurium centre also provides tellurophene with unique redox chemistry.[33] We studied the redox behaviour of 2,5-diphenyltellurophene. Under anodic oxidation, solvent molecules and/or anions coordinated to Te with oxidation confined to the Te centre, whilst under weakly coordinating conditions oxidation is delocalised over the entire π-system. In other studies, we have also observed the formation of stable hypervalent Te(IV) state from reactions of π-extended tellurophenes with different oxidants, made accessible by the metalloid nature of Te.[34–37]

Kristen L. Perry

Kristen Perry grew up in Pickering, ON and completed her B.Sc. at Western University in Integrated Science with a Chemistry specialization in 2019. Her honours thesis focused on synthesizing organometallic compounds for the reduction of carbon dioxide using secondary coordination sphere effects under the supervision of Prof. Marcus Drover. She is currently a graduate student in the Seferos group exploring modifications of biodegradable polymers for use in energy storage applications. Outside of the lab, she loves baking, painting, and playing games with friends.

Dwight S. Seferos

Dwight Seferos is a Professor of Chemistry and Professor of Chemical Engineering and Applied Chemistry at the University of Toronto. Research in the Seferos group concerns the design, synthesis, characterization, and device engineering of organic materials and polymers for electronic and optical applications. Much of their work focuses on the creation of new matter that can be used in a range of devices (OLEDs, solar cells, batteries, thermoelectrics, etc.) often leading to a wide range of highly collaborative research activities with diverse groups throughout the world.

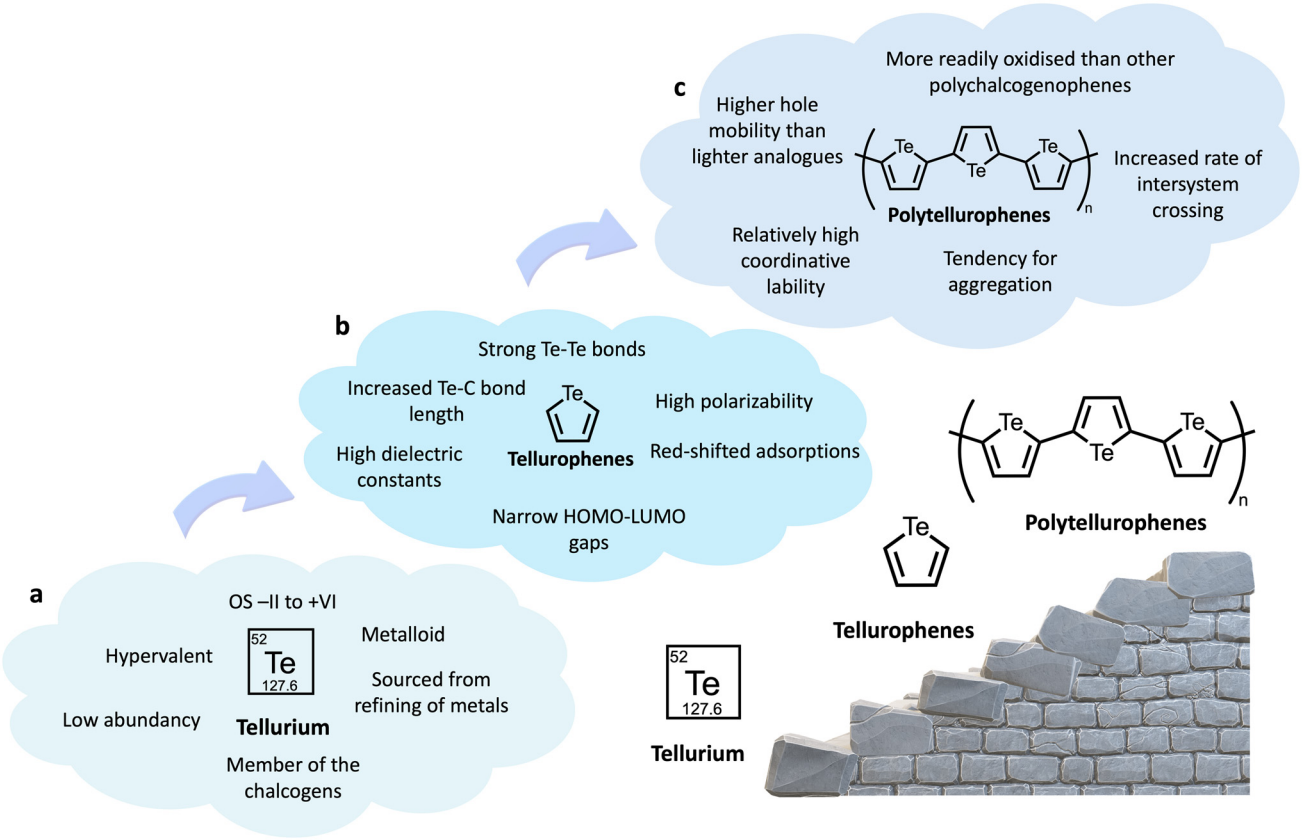

Fig. 1 Schematic and summary of the key properties of tellurium, tellurophene and polytellurophene. Properties are listed building up by size starting at (a) atomic scale tellurium then (b) heterocyclic tellurophene and then (c) polymeric polytellurophene.

Some tellurophene derivatives also have biological activity.[38] The Nitz group has employed a tellurophene-based phenylalanine (TePhe) analogue which acts as a probe in complex biological samples by fluorescent labelling by a cycloaddition reaction.[39] Previously the group has also used the TePhe to monitor protein synthesis *in vivo* with mass cytometry (Fig. 2).[40] Tellurophene substitution to the chemotherapeutic teniposide was also used to mimic the parent teniposide to monitor cell uptake by mass cytometry.[41] The Thomson group has also demonstrated that tellurophenes appended with boron-dipyrromethene dye (BODIPY) could be used as photodynamic-therapy–mass-cytometry theragnostic agents,[42] and potentially as photosensitisers for use in photodynamic therapy.[43]

2.3. Polytellurophenes

Polytellurophenes (PTes) (Fig. 1c) are conjugated polymers of repeating tellurophene monomers. Compared to their lighter polychalcogenophenes, PTes display novel properties mostly owing to the distinctive metalloid nature of tellurium. An increased rate of intersystem crossing (ISC) is observed for PTes,[22,44,45] promoted by the incorporation of the heavy tellurium atom. This attractive feature has seen tellurophene-containing semiconducting polymers being incorporated as inorganic photodynamic nano agents (section 5).[46]

The hypervalency of Te at the centre of the heterocyclic monomer also enables coordination of species by complexation which can modulate their optoelectronic properties (section 4) through variation of the electronic distribution within their π-conjugated system.[34] The lengthened C–C bond inter-ring distances[47] observed in PTes results in narrowed HOMO–LUMO gaps (optical band gap ~1.4 eV)[48] which also enriches these materials in optoelectronic applications. The strong Te–Te interactions, originating from the tellurophene monomers, leads to aggregation of PTes and low solubility,[22] and in turn affect optical and electrochemical properties.[49] Some of these properties are evidenced by a low energy absorption in the optical spectrum and irreversible shoulders in the cyclic voltammetry (CV) of tellurophene-containing cyclopentadithiophene polymer, respectively. Aggregation can also be induced by annealing and can modulate the band-gap of tellurophene containing polychalcogenophenes.[45] PTes also have a higher degree of planarity and a significant rotational barrier (compared to other polychalcogenophenes), confining their internal rotation,[50] which enhances their charge carrier mobility, for example, in field effect transistors (section 4). Additionally, regioregular 3-alkyl PTes crystallise and organise in the solid state in a distinct manner.[51]

PTes have an oxidation potential ~0.2 eV higher than PThs and are able to be more readily oxidised.[52,53] Utilisation of this

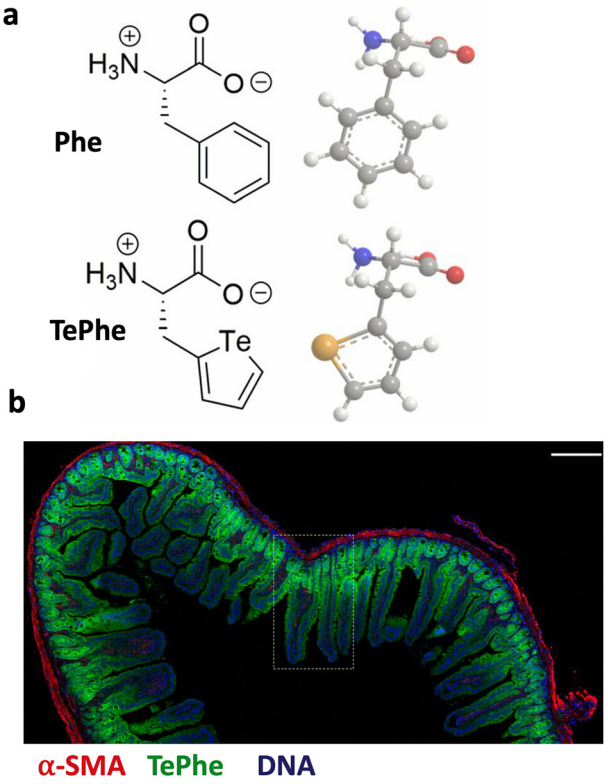

Fig. 2 Application of tellurophene in mass cytometry. (a) Chemical and density functional theory (DFT)-calculated structures of phenylalanine (Phe) and 2-tellurienylalanine (TePhe). (b) Imaging mass cytometry (IMC) demonstrating incorporation of tellurium into macromolecular structure after mouse was treated with TePhe (60 mg kg^{-1}). IMC image of the jejunum (region of small intestine) shows DNA, alpha smooth muscle actin (α-SMA) and TePhe. Strong Te signals are observed towards the tips of the finger-like structure of the cell. Scale bar = 200 μm. Reproduced from ref. 40 with permission from the National Academy of Sciences, copyright 2019.

oxidation can improve the charge-transport properties,[54] by inducing cation delocalisation across the backbone. Our group has demonstrated that selective chemical oxidation of a single block of a conjugated block copolymer can induce reversible self-assembly of oxidised micelles. This selective oxidation of a single block in the copolymer is only achievable due to the difference in oxidation potential between PTes and PThs, demonstrating the significant impact the presence of a single Te atom can make.[53]

Much of the significant developments of PTes over the past few decades since the first report of an insoluble powder by Tsukagoshi in 1985 has been summarised (Fig. 3).[55] Some of these highlights include; the first soluble PTe, a poly(arylenevinylene) from the Wittig reaction of a tellurophene dialdehyde and a phenyl diphosphonium salt;[56] a PTe copolymer with tellurophene-containing hybrid terchalcogenophenes (thiophene and selenophene);[57] a series of solution processable poly(3-alkyltellurophene)s by Kumada catalyst-transfer polymerisation (KCTP);[48] the first three-dimensional organic framework containing tellurophene;[58] and the first example of a poly(3-aryltellurophene) with narrow HOMO–LUMO gaps calculated as (E_g) = 1.3 eV.[59] Details of these synthetic milestones are discussed further in section 3 of this review.

3. Synthesis of tellurophenes, polytellurophenes and tellurophene-containing polymers

PTes are perhaps the most challenging polyheterocycles to synthesise compared to their lighter chalcogenophene analogues (furans, thiophenes, selenophenes). The main obstacle in synthesising PTes lies in the difficulty of preparing monomers that are stable, processible, and suitable for polymerisation. To overcome these synthetic challenges, researchers have developed many strategies such as the installation of side groups on tellurophene monomers and copolymerisation with solubilising monomers to enhance solubility, thermal stability and access to PTes. An interesting example of this can be demonstrated using 3-alkyltellurophene synthesis. By simply reversing the synthetic strategy from our reports of a "side chain first" to a "heterocycle first" approach, the number of synthetic steps can be reduced with a potential to access to a wide range of further modified tellurophene structures (Fig. 4).

3.1. Homopolymerisation of tellurophenes

Methodologies developed for the synthesis of PTes or tellurophene containing polymers include: electrochemical[60] or chemical[55] oxidation, cross-coupling based polymerisation reactions, or post-polymerisation element transformation. Early reports of tellurophene homopolymerisation date back to 1985 and were only obtained by oxidative polymerisation. The first such example of chemical homopolymerisation of tellurophene was reported by Tsukagoshi using $FeCl_3$ catalyst resulting in PTe (**P1**) that was insoluble in common organic solvents.[55] Another early report of PTe was by Ogura and coworkers in 1995.[61] They studied the electropolymerisation of 2,2′-bitellurophene and observed the formation of PTe (**P2**) as a black powder or film. In 2009, Bendikov and coworkers synthesised the first substituted tellurophene homopolymer (**P3**) through electropolymerisation, however, this species suffered from low stability compared to the Se counterpart[62] (Fig. 5).

In 2013, our group reported the first homopolymerisation of 3-alkyl tellurophenes by both electrochemical and chemical polymerisation.[48] 3-Alkyltellurophene monomers were synthesised by a ring-closing reaction. First, the Weinreb amide 2-chloro-*N*-methoxy-*N*-methylacetamide (**1**) was treated with a Grignard reagent to afford the corresponding 1-chloro ketone (**2**). This ketone can be treated with ethynyl magnesium bromide, followed by sodium telluride solution to afford the five-membered tellurium-containing ring (**4**). Dehydration then provides 3-alkyl substituted tellurophenes (**5**) for the first time (Fig. 4a).

Diiodo monomers were then synthesised by the reaction of 3-alkyl tellurophenes with *sec*-butyllithium followed by iodine

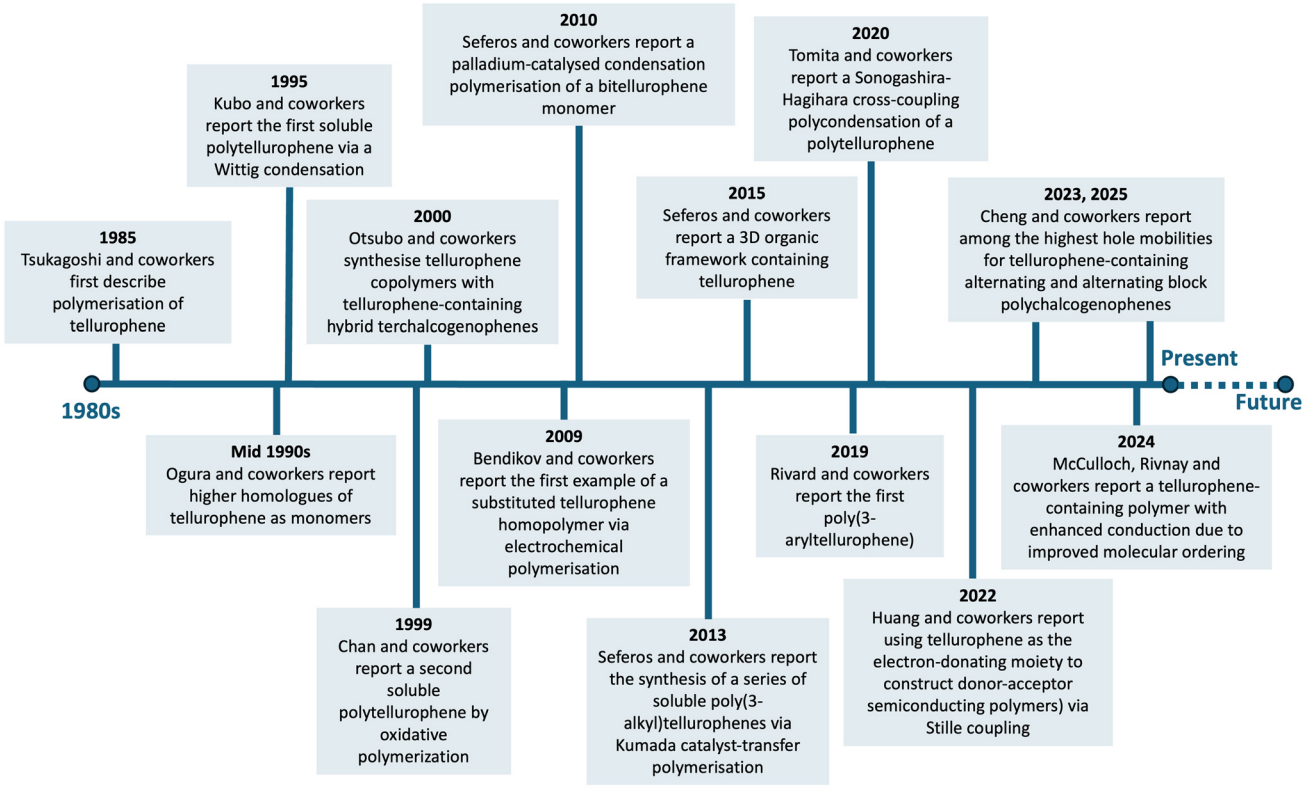

Fig. 3 Timeline for major developments in the preparation of polytellurophenes over the past few decades.

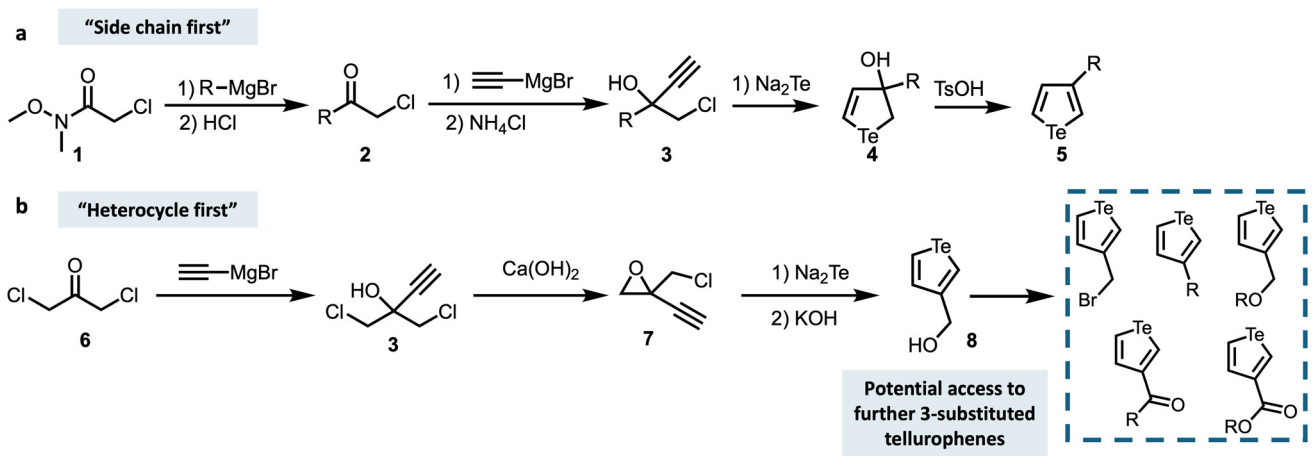

Fig. 4 Methods to synthesise substituted 3R-tellurophenes.[60] (a) Reported synthetic procedure for the synthesis of 3-alkyl tellurophenes in which the ring-closing precursors bearing the side chains need to be first synthesised. (b) Synthesis of a 3-hydroxymethyltellurophene which can offer potential access to further 3-substituted tellurophenes, reducing the number of synthetic steps.[61]

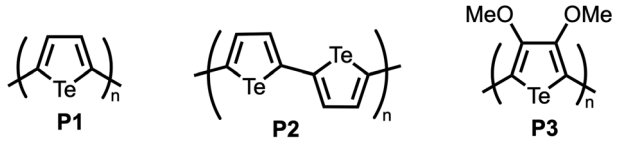

Fig. 5 Structures of the earliest reported PTes homopolymers.

(early attempts at NBS-type halogenation all failed in our hands, although this would eventually be overcome).[63] Treatment of halogenated monomers under Kumada Catalyst-Transfer Polymerisation (KCTP)[64] conditions yielded poly(3-alkyl tellurophene)s (**P4**) (Fig. 6) with M_n = 5.4 kDa–11.3 kDa and $Đ$ = 1.9–2.2 depending on the alkyl substituent.

The obtained polymers had broad $Đ$ and lower than expected molecular weights, indicating that standard KCTP

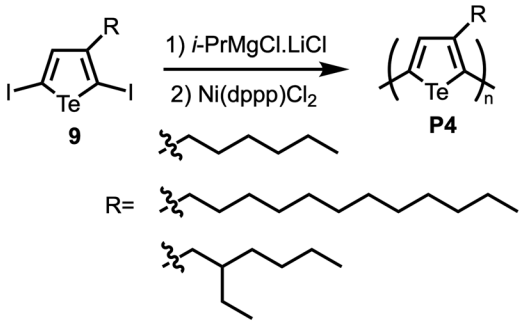

Fig. 6 Homopolymerisation of 3-alkyl tellurophenes; dppp = 1,3-bis (diphenylphosphino)propane.

conditions did not produce polymers in a controlled manner (at least initially). However, this homopolymerisation method was significant because it opened doors to soluble tellurophene homo- and co-polymerisation and higher molecular weight polymers.[50,65]

Later, we systematically examined the effects of polymerisation conditions and monomer design through experimental and computational studies. We showed that increasing the length of the linear side chain increases the polymer molecular weight without changing the dispersity.[65] This observation showed that the formation of higher molecular weight polymers may be limited by solubility. Additionally, optimising the branching point within the alkyl chain moiety showed that the branched side chains that were required for solubility also affected the polymerisation kinetics. Branching beyond the 3-position does not significantly affect the polymerisation kinetics. Through these investigations, we developed rationally designed 3-alkyl tellurophene monomers to access polymers with high molecular weights (M_n = 24.9 kDa), narrow dispersities, and well-defined end groups.

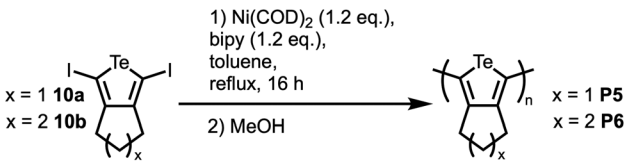

Fig. 7 Oligomerisation of (cyclo)tellurophenes.

Sang, Rivard, and coworkers demonstrated the formation of oligomeric (cycloalkyl)tellurophenes from iodinated tellurophene building blocks.[59] Attempts to homopolymerise 2,5-iodinated tellurophenes by Yamamoto coupling in the presence of stochiometric $Ni(COD)_2$/bipy (bipy = 2,2′-bipyridine; COD = 1,5-cyclooctadiene), formed (cyclo)tellurophene oligomers (**P5** and **P6**) (Fig. 7). The authors mentioned that low solubility prevented the formation of high molecular weight polymers in this system. The monomer with tellurophene fused to the cyclohexane ring (**10b**) formed longer chain oligomers than the tellurophene fused to the cyclopentane ring (**10a**), perhaps due to greater solubility caused by enhanced backbone ring twisting in **P6**.

The same group of investigators also installed a cumenyl group on a tellurophene molecule by Suzuki–Miyaura coupling to form a 3-arylated tellurophene (**13**).[59] This arylated tellurophene was iodinated at the 2-and 5-positions to produce diiodinated tellurophene (**14**) as the monomer. KCTP polymerisation of **14** yielded the first reported poly(3-aryltellurophene) (**P7**) (Fig. 8).

In 2021, Rivard and coworkers reported the synthesis of telluro(benzo)bithiophenes using zirconium-mediated alkyne coupling and Zr–Te atom exchange.[66] Following the synthesis of tellurium compound (**15**) and its dibrominated analogue (**16**), they performed homopolymerisation using KCTP methods and obtained the unstable oligomeric material, (**P8**) (Fig. 9). This example demonstrates the polymerisation of a fused, conjugated tellurophene/thiophene monomeric unit.

In another report, our group studied the effect of halogen and magnesium salts in KCTPs and showed that the halogen

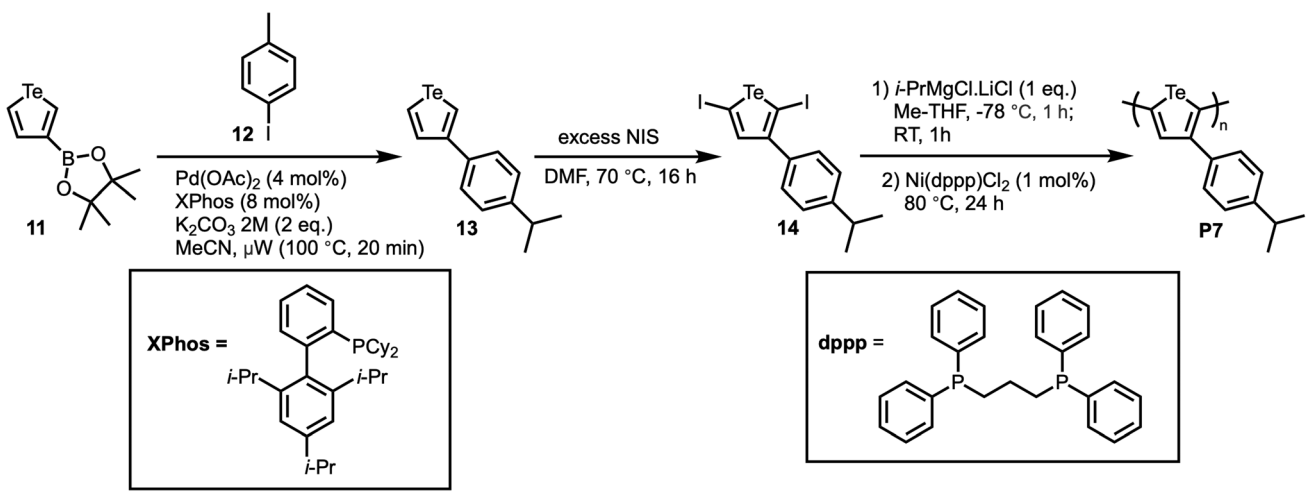

Fig. 8 Synthesis and polymerisation of 3-aryl tellurophenes. NIS = *N*-iodosuccinimide.

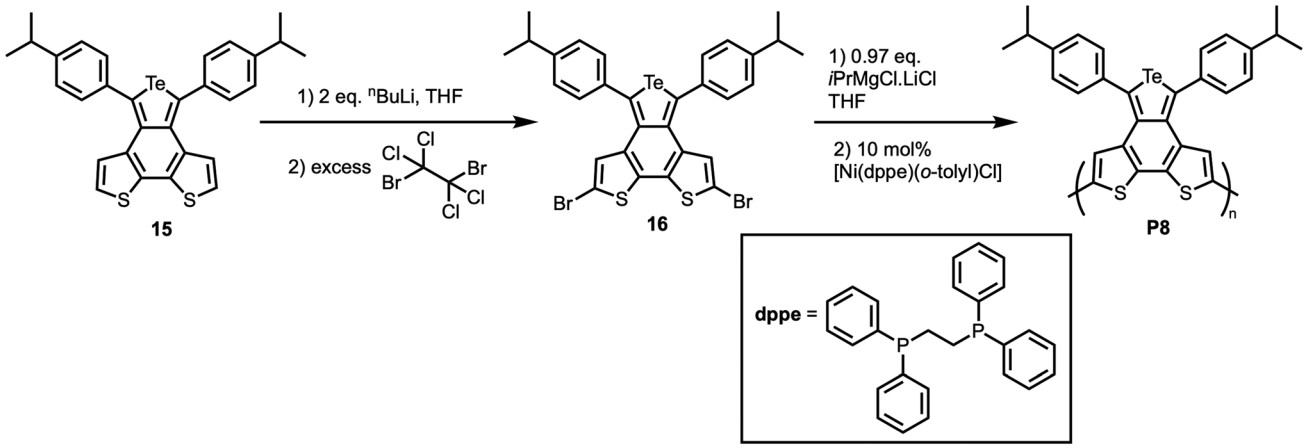

Fig. 9 Oligomerisation of telluro(benzo)bithiophenes. dppe = 1,2-bis(diphenylphosphino)ethane.

atom plays an important role in the kinetics and living nature of the polymerisation.[67] With this knowledge, we demonstrated the first synthesis of a poly(3-(2-ethylhexyl)tellurophene) (**P4**) bearing a bulky side chain with M_n = 8.4 kDa and $Đ$ = 1.2 (Fig. 10). The increase in the molecular weight of this polymer compared to previous studies[48] is due to the use of bromo-iodo-tellurophene (**17**) as opposed to diiodo-tellurophene (**9**). This example highlights the importance in the of selection of halogen atoms, especially for monomers with bulky side chain groups.

3.2. Copolymerisation of tellurophenes

One strategy to improve the solubility and processibility of PTes is the copolymerisation with more soluble monomers. Many synthetic strategies have been used for incorporating tellurophene monomers in polymer structures, such as Wittig condensation, oxidative polymerisation, Suzuki, Sonagashira and Stille-type cross-coupling reactions. The first soluble tellurophene-containing polymer was synthesised through a Wittig condensation reaction between tellurophene dialdehyde (**18**) and a phenyl diphosphonium salt to yield (**P9**) (Fig. 11a).[56] Another early report of tellurophene polymerisation was the oxidative polymerisation of a thiophene–tellurophene–thiophene ter-monomer using $FeCl_3$ (**P10**) (Fig. 11b).[68]

Multiple examples of Suzuki–Miyaura and Sonagashira cross-coupling reactions have been employed (Fig. 12). In 2010, our group demonstrated the synthesis of poly(bitellurophene-*alt*-9,9′-dihexylfluorene) (**P11**) by Suzuki-type polymerisation.[34] The choice of 9,9-dihexyl-fluorene comonomer increased the solubility of the resulting polymer. Indeed, the resulting polymer was soluble in common organic solvents such as THF, chloroform, and chlorobenzene. Halogenation of bitellurophene (**21**) at the 5 and 5′ positions was achieved by using *N*-iodosuccinimide (NIS) to afford the diiodo monomer (**22**) (Fig. 12a). The optimised procedure for polymerisation involved the biphasic reaction of a boronic ester and 5,5′-diiodo-2,2′-bitellurophene (**22**) in the presence of Pd catalyst, a phase-transfer agent Aliquat 336, and aqueous K_2CO_3 base to yield the copolymer **P11** with M_n of 3.1 kg mol^{-1} and $Đ$ = 1.2.

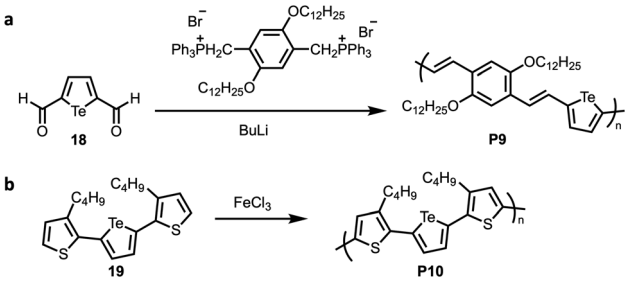

Fig. 11 Methods of copolymerisation of tellurophene monomers by (a) Wittig condensation with a diphosphonium salt and (b) electro-polymerisation with a thiophene block.

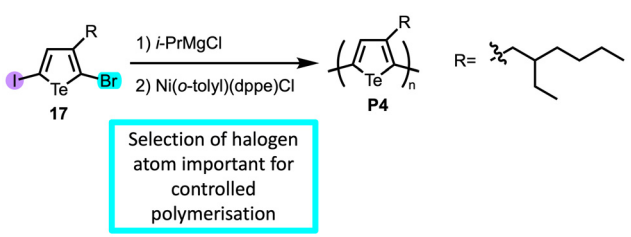

Fig. 10 Homopolymerisation of 2-bromo, 5-iodo-3-(2-ethylhexyl) tellurophene.

Rivard and coworkers showed the synthesis of tellurophene–thiophene copolymer and thiophene–selenophene–tellurophene copolymer.[69] In their system, they implemented Zr-mediated metallacycle transfer chemistry to access heterocycle monomers, followed by Suzuki–Miyaura cross-coupling polymerisation to synthesise tellurophene-containing polymers. This Zr-mediated metallacycle transfer chemistry has also been used in other systems to generate Te-containing rings.[70–72] Reaction of the zirconacycle (**23**) with an appropriate chalcogen halide generates the desired chalcogenophene with pinacolboronate (BPin) cross-coupling groups at the 2- and 5-positions (**24**) (Fig. 12b). 2,2′-Bipyridyl-sequestered tell-

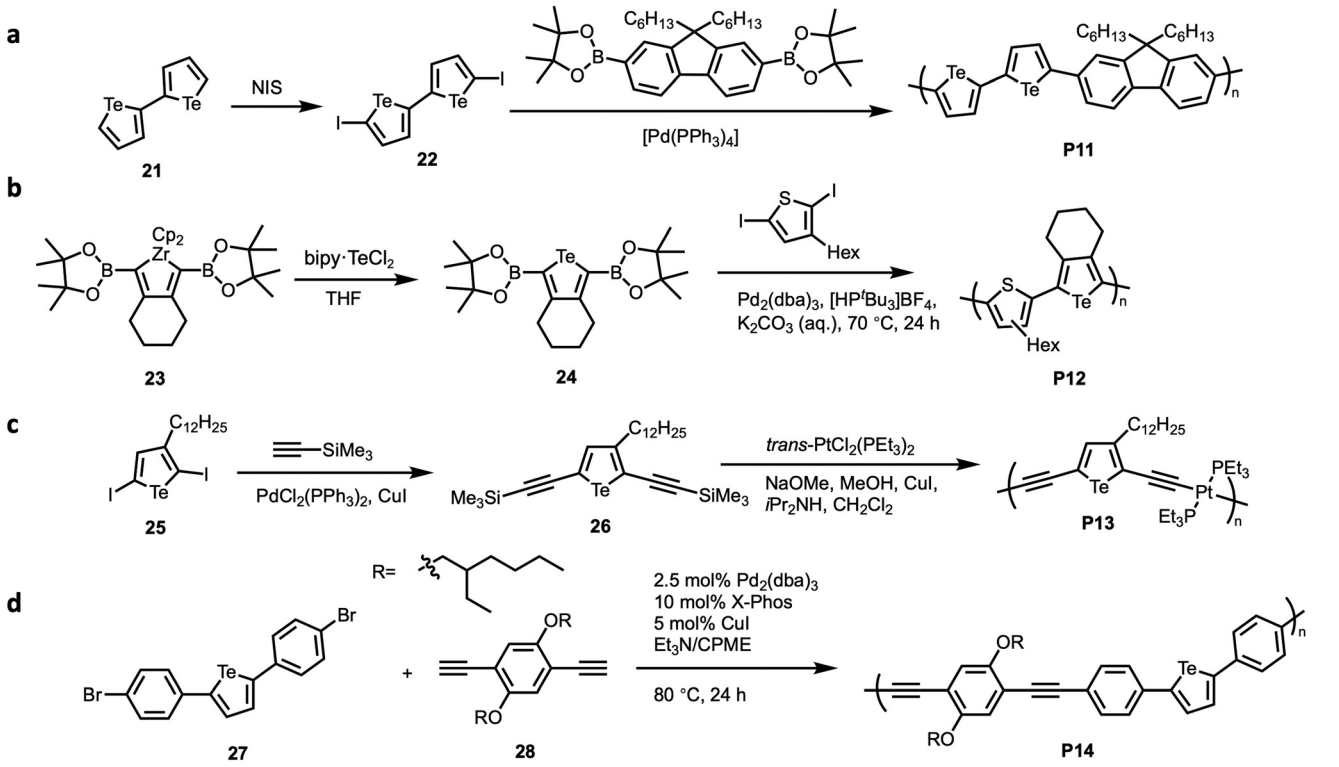

Fig. 12 Examples of Suzuki–Miyaura and Sonagashira–Hagihara type cross couplings for the copolymerisation of tellurophene monomers. Copolymerisation of (a) bitellurophene and a fluorene derivative, (b) 2,5-dibromo-3-hexylthiophene and a tellurophene heterocycle formed by zirconacycle transfer chemistry, (c) 3-alkyl tellurophene with platinum-acetylide, and (d) 2,5-di(4-bromophenyl) tellurophene and an arylene dibromide. dba = dibenzylideneacetone.

urium dihalide adduct (bipy·$TeCl_2$) was chosen as the tellurium source. The resulting tellurophene (**24**) showed high thermal stability. Following this monomer synthesis, Suzuki-cross coupling with 2,5-dibromo-3-hexylthiophene resulted in regio-random copolymers of thiophene and tellurophene (**P12**) with M_n of 3.6–6.5 kg mol^{-1}.

The copolymerisation of 3-alkyl tellurophene with platinum-acetylide was reported by our group in 2016 for their photophysical properties.[73] In this work, we showed that the treatment of halogenated tellurophene (**25**) with trimethylsilylacetylene under Sonogashira coupling conditions produces the 2,5-bis(trimethylsilylethynyl)-3-dodecyl tellurophene monomer (**26**) (Fig. 12c). Subsequently, the reaction of this monomer (**26**) with sodium methoxide, methanol, and *trans*-bis(triethylphosphine)platinum(II) dichloride under an inert atmosphere produced the desired copolymer of tellurophene with platinum–acetylide (**P13**).

A final report for the incorporation of tellurophenes in polymers by Sonagashira–Hagihara cross-coupling was in 2020 by Tomita and coworkers.[74] They synthesised tellurophene-containing polymer (**P14**) with M_n = 2.7 kg mol^{-1} and $Đ$ = 1.80 using an arylene dibromide (**27**), a diyne (**28**), and a palladium catalyst (Fig. 12d).

Stille couplings have also been explored (Fig. 13). Heeney and coworkers showed copolymerisation of dibrominated 3-dodecyltellurophene (**29**) with (*E*)1,2-bis(tributylstannyl) ethylene using Stille cross-coupling to afford poly(3-dodecyl-2,5 tellurophenylenevinylene), (**P15**) (Fig. 13a), which is an early example of a donor–acceptor polymer that contains tellurophene.[75] In this system, the tellurophene-based monomer is the halide coupling partner and the alkene-based monomer is the *trans* stannylated vinyl compound. Stille cross-coupling has also been used to form copolymers of tellurophenes, with tellurophene-based monomer as the tin-containing reagent.

Choi and coworkers showed the polymerisation of a diketopyrrolopyrrole (**30**) with tellurophene monomer by Stille coupling in the presence of tetrakis(triphenylphosphine)palladium (0) catalyst to afford copolymer of tellurophene and diketopyrrolopyrrole (**P16**) with M_n of 53.7 kg mol^{-1} and $Đ$ = 2.49 (Fig. 13b).[76] Similarly, Ashraf and coworkers synthesised copolymers of a diketopyrrolopyrrole-based monomer (**31**) with a tellurophene monomer through microwave-assisted Stille coupling (Fig. 13c).[77] Jo and coworkers used Stille coupling to synthesise a copolymer of an isoindigo-based monomer and tellurophenes (**P18**) with M_n = 47 kDa and $Đ$ = 1.60 (Fig. 13d).[78] A recent study also used Stille coupling to prepare alternating copolymers of oligo-ethylene glycol substituted-bithiophene with tellurophene (**P19**) in the presence of $Pd_2(dba)_3$ and P(*o*-anisyl)$_3$ catalyst (Fig. 13e).[79]

In 2015, our group synthesised a three-dimensional (3D) aromatic framework incorporating tellurophenes.[80] This tellurophene-containing 3D framework was made through the Stille

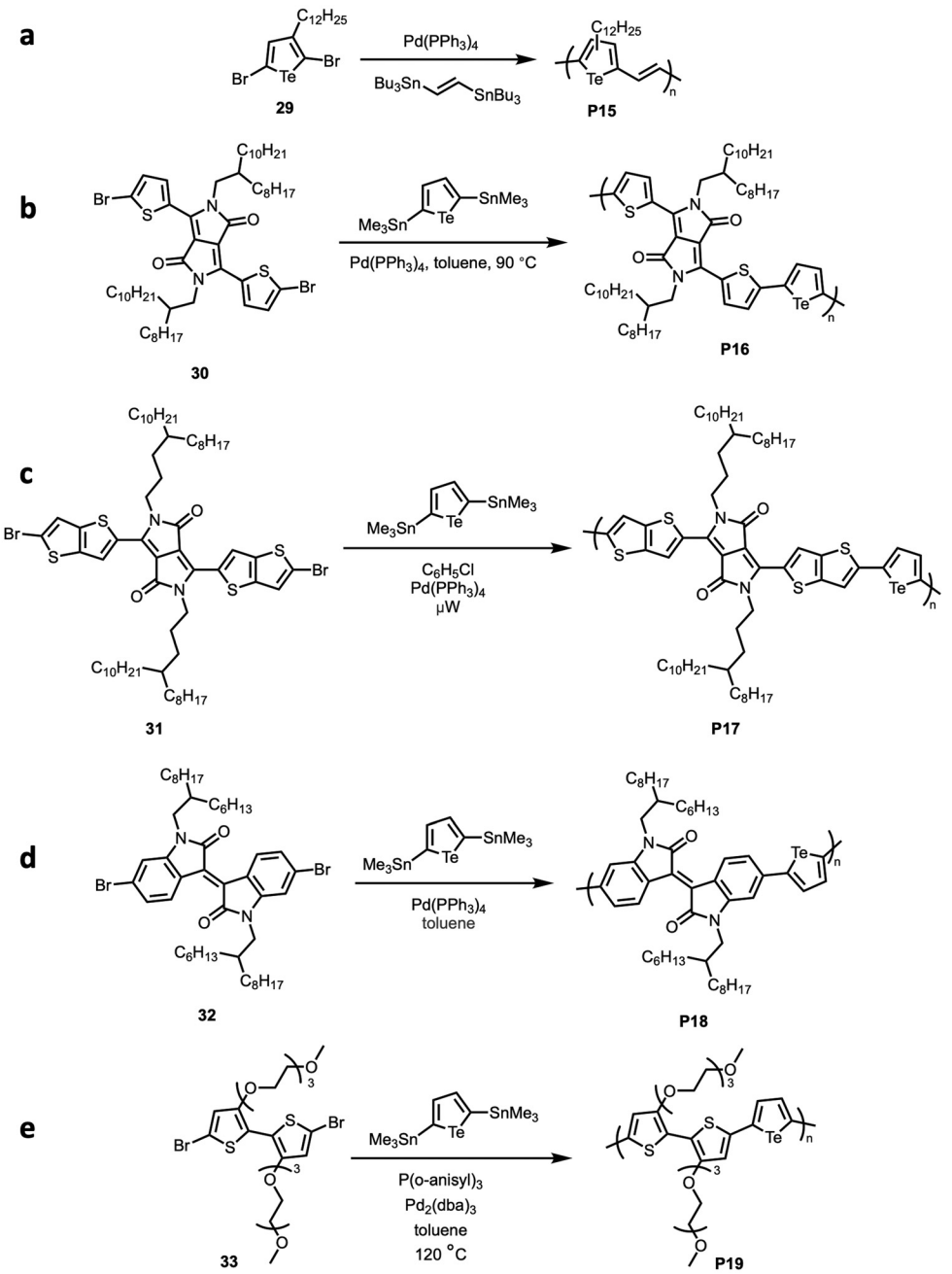

Fig. 13 Examples of the copolymerisation of tellurophenes by Stille coupling. (a) Copolymerisation of 3-dodecyltellurophene with tin-containing alkene. (b)–(d) Copolymerisation of tin-containing tellurophene monomer with diketopyrrolopyrroles. (e) Copolymerisation of oligo-ethylene glycol substituted-bithiophene with tin-containing tellurophene monomer.

coupling of 1,3,5,7-tetrakis(4-iodophenyl)adamantane (**34**) and the 2,5-bis(trimethyltin)tellurophene (Fig. 14).

Further methods of copolymerisation have also been explored such as *ipso*-arylative copolymerisation, direct heteroarylation polymerisation (DHAP), and Kumada catalyst transfer polycondensation (KCTP) which circumvent tin-containing monomers (Fig. 15). Grubbs and coworkers used Pd-catalysed *ipso*-arylative copolymerisation of a tellurophene monomer (**35**) with a diketopyrrolopyrrole (dpp) (**30**) to generate tellurophene-dpp copolymer, **P16** (Fig. 15a).[81] In this approach, the organic benzophenone leaving group enables coupling reactions without generating stochiometric amounts of organometallic by-products, such as trialkyltin halides as seen in previously mentioned reports for the same polymer (Fig. 13b). This method generated the tellurophene-containing polymer (**P16**) as a mixture of a low molecular weight fraction (M_n = 8.0 kg mol^{-1} and $Đ$ = 3.8) and a higher-molecular weight fraction (M_n = 23.2 kg mol^{-1} and $Đ$ = 3.7). Additionally, the

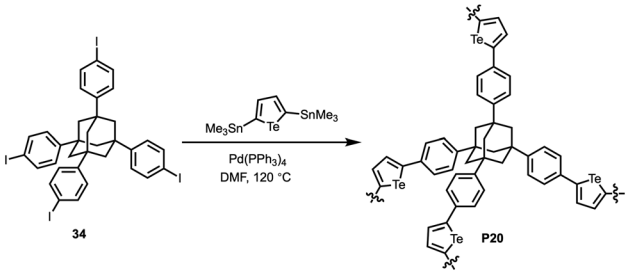

Fig. 14 Synthesis of tellurophene-containing 3D framework by Stille coupling.

authors reported stability of the monomer for up to one year after its initial synthesis.

In 2019, Hu, Huang and coworkers synthesised copolymers of naphthalene diimide (NDI) (**36**) and bitellurophene (**21**) by direct heteroarylation polymerisation to form NDI-*co*-bitellurophene (**P21**, Fig. 15b).[46] This approach was chosen for its higher atom economy and lower toxicity compared to couplings employing organotin reagents. Additionally, authors noted that attempts to stannylate or borylate the bitellurophene comonomer failed.

In 2020, Cheng and coworkers designed unsymmetrical diiodobichalcogenogene monomers to form alternating copolymers of thiophene–tellurophene and selenophene–tellurophenes.[82] Diiodobichalcogenogene monomers were first prepared (**39** and **41**) and were treated with ^{i}PrMgCl·LiCl and Ni-catalysed KCTP forming selenophene-*alt*-tellurophene copolymer (**P22**) and thiophene-*alt*-tellurophene copolymer (**P23**) (Fig. 15c and d). Similarly, a pre-sequenced monomer consisting of thiophene, selenophene, and tellurophene (**45**) was prepared to form the first reported alternating regioregular poly (terchalcogenophene) (**P24**) (Fig. 15e). Although the polymerisation was performed using KCTP conditions, Stille coupling of selenophene, thiophene and tellurophene units, were required to form the desired diiodobichalcogenogene monomers **39**, **41** and **45**.

In subsequent reports by the same group,[83,84] KCTP was also employed for the formation of alternating block conjugated copolymers. In 2023, sequence-controlled polychalcogenophenes were synthesised with general formula poly(*alt*-AB)$_x$-*b*-(*alt*-AC)$_y$, where A, B and C were either 3-hexylthiophene, 3-hexylselenophene or 3-hexyltellurophene.[83] These polymers were prepared with high side-chain regioregularity. In 2025, similar polymers were synthesised instead keeping one block as poly (3-hexylthiophene) (P3HT), to improve crystallinity.[84] These polymers were denoted poly(*alt*-AB)*b*(3HT), where A and B were also either 3-hexylthiophene, 3-hexylselenophene, or 3-hexyltellurophene. These examples also required the use of alkyl tin species for monomer formation.

Tellurophenes have been incorporated in viologen small molecules multiple times in the literature by the He group.[85–89] In 2019, He and coworkers attempted to synthesise poly(chalcogenoviologen) by the nucleophilic substitution reaction of a,a′-dibromo-*p*-xylene with a tellurophene-bridged viologen molecule (**46**).[90] However, they only obtained low molecular weight xylylviologen oligomers of 12 repeat units (**P25** and **P26**, Fig. 16).

3.3. Post-polymerisation modifications

Tellurophene-containing polymers can also be accessed by post-polymerisation methods (Fig. 17). Our group reported the synthesis of tellurium-containing polymers by post-polymerisation modifications that exchange Se for Te.[91] This process reduces a selenium benzoselenadiazolepolymer (**47**) into its diamino along (**48**) using $LiAlH_4$. The diamino containing-polymer was then re-oxidised with tellurium tetrachloride to incorporate Te in the diazo moiety, resulting in the benzotellurodiazole polymer (**P27**) (Fig. 17a).

Tomita and coworkers showed another element transformation post-polymerisation pathway to synthesise a PTes.[92] Inspired by other studies exhibiting the conversion of zirconacycles into tellurophenes and similar reactivity of titanacyclopentadiene derivatives to their zirconacyclopentadienes analogues, the authors showed conversion of organotitanium polymer (**49**) to tellurophene-containing polymer (**P28**) (M_n = 5.1 kg mol^{-1} and $Đ$ = 2.4). This transformation was performed using $TeCl_4$ as the Te reagent at low temperature, followed by reduction using sodium thiosulfate solution (Fig. 17b).

Parent PTes can also undergo post-polymerisation element transformations to form alternative polymers (Fig. 18). Tomita and coworkers showed that reacting tellurophene containing polymers (**P29** and **P14**) with *n*-butyllithium produces lithiated intermediates (**50** and **51**) as powerful synthetic precursors, which react with various species to produce tin-containing[93] (**P30**) and germanium-containing[74,94] (**P31** and **P32**) polymers.

These examples demonstrate the progress made since the first reports of insoluble, low molecular weight and/or high $Đ$ PTes. The synthetic toolbox has been greatly expanded upon to allow for a more diverse range of synthetic strategies resulting in the synthesis of tellurophene monomers and resultant PTes or tellurophene-containing polymers that have more favourable properties. Methods to overcome inherent solubility issues, such as the installation of side groups on tellurophene monomers and copolymerisation with solubilising monomers, have been addressed to allow access to higher-functionality complex structures.

Despite these advances, PTes synthesis still has challenges related to the sustainable and scalable synthesis of these materials. We have discussed several methods to prepare tellurophene-based polymers that often use toxic solvents, harmful reagents, and harsh reaction conditions. Indeed, one of the most frequently employed strategies discussed is Stille-type couplings, which use inherently toxic organostannane monomers. This poses issues for any potential industrial or device applications. Additionally, some of the methods of preparation for other polychalcogenophenes have not yet been successfully applied to PTes. One such example is the Suzuki–Miyaura Catalyst-Transfer Polymerisation (CTP) for the synthesis of PTes homopolymers that has allowed for the controlled polymerisation of both electron-rich and electron-

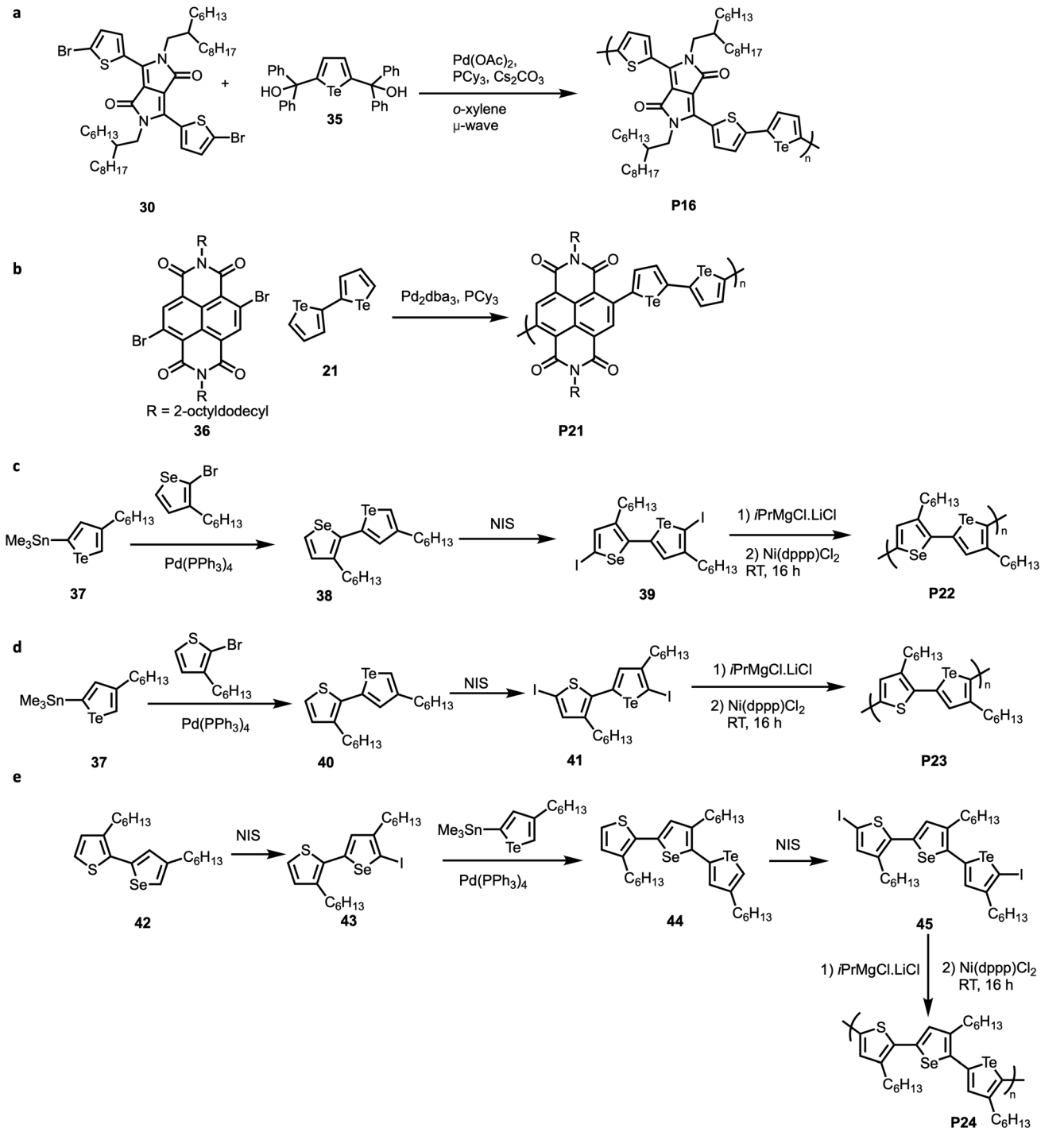

Fig. 15 Alternative copolymerisation methods of tellurophene-containing monomers. (a) *ipso*-Arylative copolymerisation, (b) direct heteroarylation polymerisation (DHAP), and (c)–(f) Kumada catalyst-transfer polycondensation (KCTP).

deficient monomers of other chalcogenophenes.[95] Direct arylation polymerisations (DArP), which proceed through a concerted metalation-deprotonation process, have recently been demonstrated to synthesise thiophene-containing polymers with few structural defects in green solvents at low temperatures (<70 °C)[96] but have not yet been applied to PTes. The inherent properties that are characteristic of PTes, such as their tendency to aggregate,[65] reduced aromaticity,[20] and the instability of tellurophene derivatives (as demonstrated by their susceptibility to oxidative ring opening),[97] further complicate the challenges of applying these conditions in attempts to control PTes polymerisation.

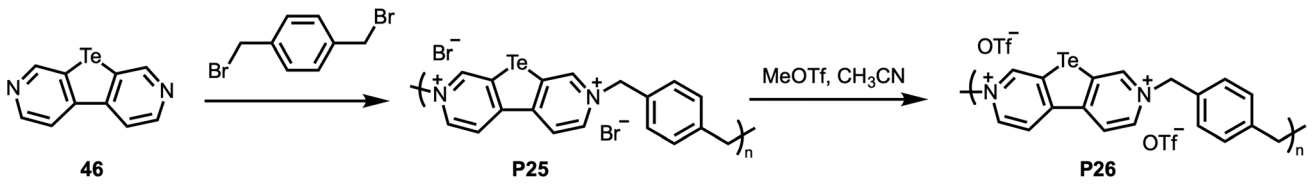

Fig. 16 Synthesis of tellurophene-containing xylylviologen oligomers.

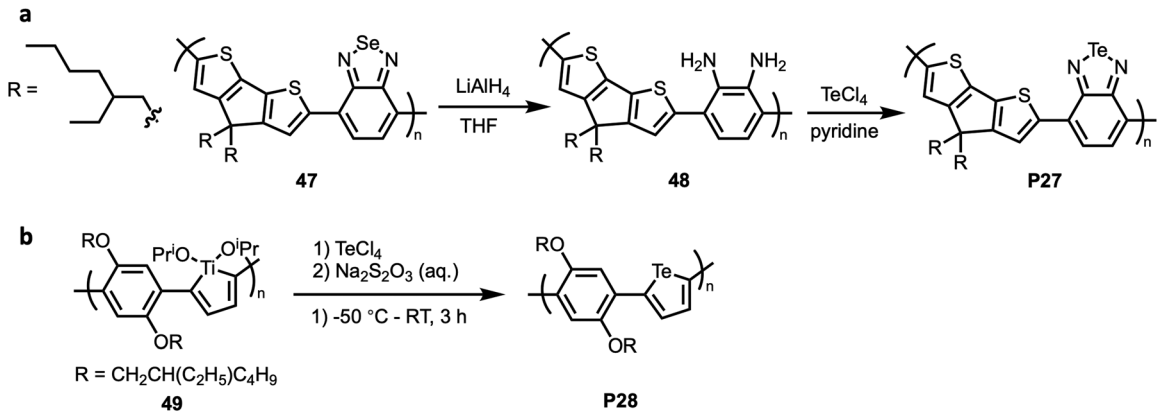

Fig. 17 Post-polymerisation methods to access tellurophene containing polymers. (a) Conversion of selenium-containing polymer to tellurium-containing polymer. (b) Conversion of titanium-containing polymer to tellurophene-containing polymer.

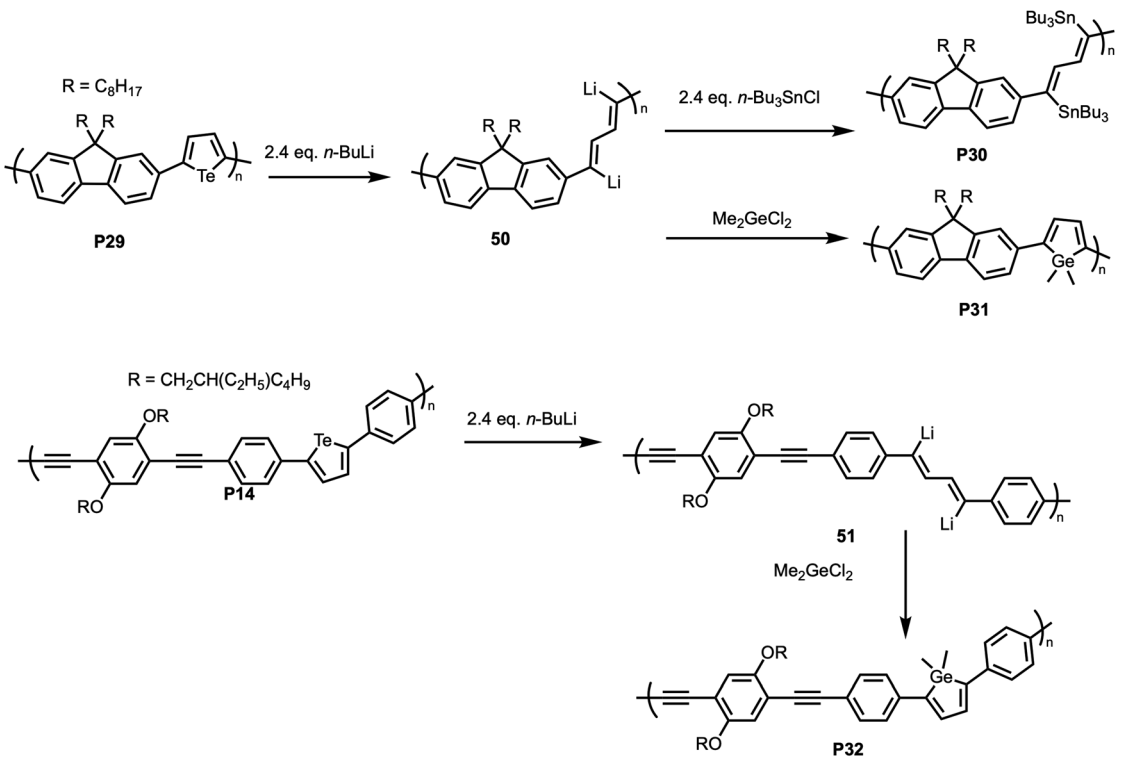

Fig. 18 Examples of post-polymerisation element transformation of PTes.

4. Optoelectronic applications of polytellurophenes and tellurophene-containing polymers

4.1. Organic solar cells/organic photovoltaics

With the growing demand for clean energy, solar power is becoming an increasingly important field of research. More specifically, organic solar cells (OSCs), also known as organic photovoltaics (OPVs), have received intense research activity, owing to the success of other industrial compounds and materials. OPV research involves the development of electron-donor and electron-acceptor pairs with an appropriate HOMO and LUMO offset to effect exciton formation and maximise spectral coverage that in turn maximise the voltage and current output from the OPVs. This topic has been extensively reviewed elsewhere.[98–102] Conjugated polymers are a promising class of materials to be used in OPV applications because of the energy level tuning that can be achieved through synthetic chemistry such as backbone and side chain modifications to the polymers. Polychalcogenophenes, most commonly PThs, or more broadly thiophenes, are a widely used class of building blocks for OPV materials. The thiophene unit is incorporated into nearly every class of donor–acceptor pairs, due to their thermal and chemical stability, ease of chemical modification, as well as their ability to harvest light efficiently, and excellent charge-transport properties.[103]

Compared to other chalcogens, tellurium has interesting properties that offer it different advantages in semiconducting polymers. As discussed in section 2, tellurium is a metalloid and, therefore, has the ability to form hypervalent bonds in charge transfer complexes, which can be used to control the properties of tellurophene-based conjugated polymers.[104] This metalloid property of tellurium could also allow these tellurophene semiconductors to populate triplet excited states by ISC.[105] These triplet excitons have longer lifetimes which should allow for longer exciton life-times and more photocurrent collection, leading to higher power conversion efficiencies.[106] Additionally, tellurophene has a narrower HOMO–LUMO gap compared to furan, thiophene, and selenophene, and comparatively, the optical absorption of tellurophene-based polymers is red-shifted, collecting more of the solar spectra.[75] More photon collection results in the increased current density for the semiconductor.[107] These characteristics and properties of tellurium make it a promising material to be used in organic semiconductors.

Grubbs and coworkers have combined bitellurophene units with a DPP units to make a conjugated polymer (PDPPTe2T, **P16**) that were tested in photovoltaic devices.[81] Compared to analogous sulfur-containing materials (PDPP3T), the tellurophene-based polymers showed better light harvesting at longer wavelengths, improving the efficiency of the solar cell material.[81] The authors also noted the importance of the polymer molecular weight on the efficiency of the solar cell material by investigating the difference of bends of high- and low-molecular-weight polymers in the devices. Density functional theory (DFT) calculations also revealed Te contributed more to the LUMO, whilst S contributed more to the HOMO (Fig. 19a).

Further studies on similar polymeric structures (DPPTT-X, where X = S, Se or Te, **P17**) that compared thiophene, selenophene, and tellurophene units in OPVs demonstrated that an increase in the chalcogen atomic size leads to a reduction in aromaticity which results in the slight raise of the HOMO energy levels and decrease in the LUMO energy levels.[77] This leads to the narrowing of the optical bandgap and red shifting of the absorption of the conjugated polymers (Fig. 19b). The heavier tellurophene also contributes to an increase in the crystallinity of the materials because of its higher polarizability

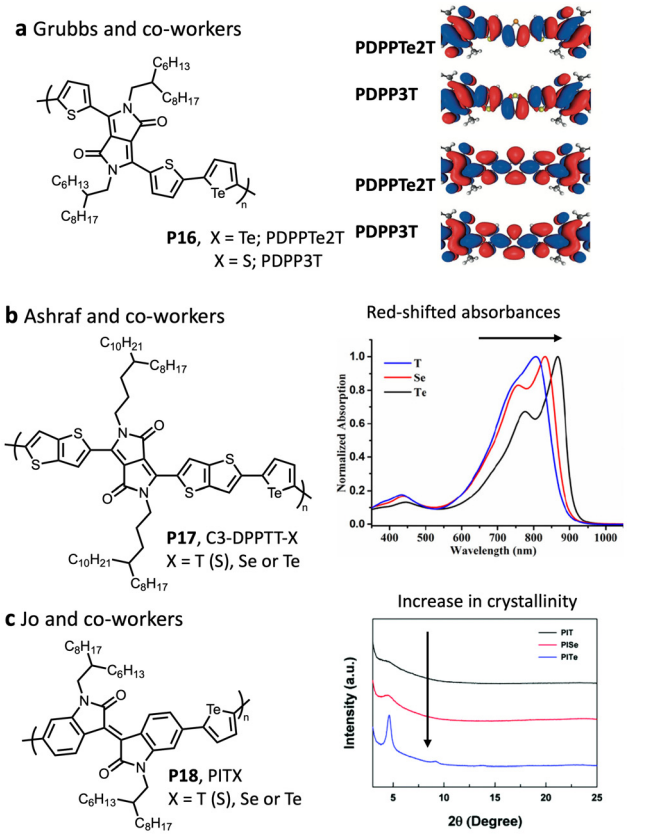

Fig. 19 Incorporation of tellurophene in conjugated polymers for organic solar cells. (a) Reports of polymer PDPPTe2T and PDPP3T by Grubbs and coworkers and calculated frontier orbitals of PDPPTe2T (top) and PDPP3T (bottom). Reproduced (adapted) from ref. 81 with permission from John Wiley and Sons, copyright 2014. (b) Reports of polymer C3-DPPTT-X, where X = S, Se or Te by Ashraf and coworkers. UV-Vis absorption profiles of polymers C3-DPPTT-T, C3-DPPTT-Se, and C3-DPPTT-Te in dilute chlorobenzene solution showing a red-shifted adsorption with increasing atomic number. Reproduced (adapted) from ref. 77 with permission from American Chemical Society, copyright 2015 (c) Report by Jo and coworkers of isoindigo-based polymers PITX, where X = S, Se or Te. X-ray diffraction patterns of the polymers in solid film demonstrating an increase in crystallinity with increasing atomic number. Reproduced (adapted) from ref. 78 with permission from Royal Society of Chemistry, copyright 2014.

and stronger intermolecular interactions, which contributes to enhanced field-effect hole mobilities.

Similar results were found in a study by Jo and coworkers comparing the same three chalcogenophene units but with isoindigo-based units to create the conjugated polymers (PITX, where X = S, Se or Te, **P18**).[78] The tellurophene-based polymer was reported to have the lowest power conversion efficiency of the three polymeric systems but displayed the highest field-effect transistor hole mobility due to the comparatively higher degree of crystallinity observed in X-ray diffraction patterns (Fig. 19c).

Tellurophene polymers have also been examined as n-type polymeric semiconductors.[108] These non-fullerene n-type materials are of interest in the search for more efficient OPVs and in the development of all-polymer solar cells. These are attractive owing to the flexibility in controlling solution viscosity to aid the solution processibility in OPV production, their adjustable energy levels, and enhanced absorption. A series of tellurophene-based polymers were constructed with perylene diimide (PDI) or naphthalene diimide (NDI) units as n-type semiconductors[109] (Fig. 20a), whilst PTB7-Th (Fig. 20b) was used as the donor for the construction of all-polymer solar cells (Fig. 20c). The NDI-based tellurophene polymers outperform the PDI-containing species in terms of cell efficiency, attributed to the increased planarity that improves π–π stacking, raises the LUMO energy, and results in better electron transport capability.[108] Modifications to the ratio of donor–acceptor (D–A), as well as the alkyl chain lengths improve the efficiency of the photovoltaic performance, which was observed in the *J*–*V* curves and external quantum efficiency (EQE) plots (Fig. 20d and e). The best performance was observed with polymeric system PTB7-Th:PTe-NDI(HD) (1 : 1.2 w/w) that reaches 4.3% power conversion efficiency.

Tuning of the band gap on the PTe backbone has been examined with cycloalkyl, as well as aryl substituents. Sang, Rivard, and coworkers determined that less sterically hindered 5-membered side groups on the tellurophene units yield a more planar backbone and result in a considerable reduction of the HOMO–LUMO gap.[59] Additionally, PTe containing aryl substituents were found to have decreased band gaps as compared to PTes and PThs with just alkyl side chains. Tellurophene-based polymers show great promise in OPV materials research, but the properties of these polymers are perhaps even more well-suited for use in field effect transistors.

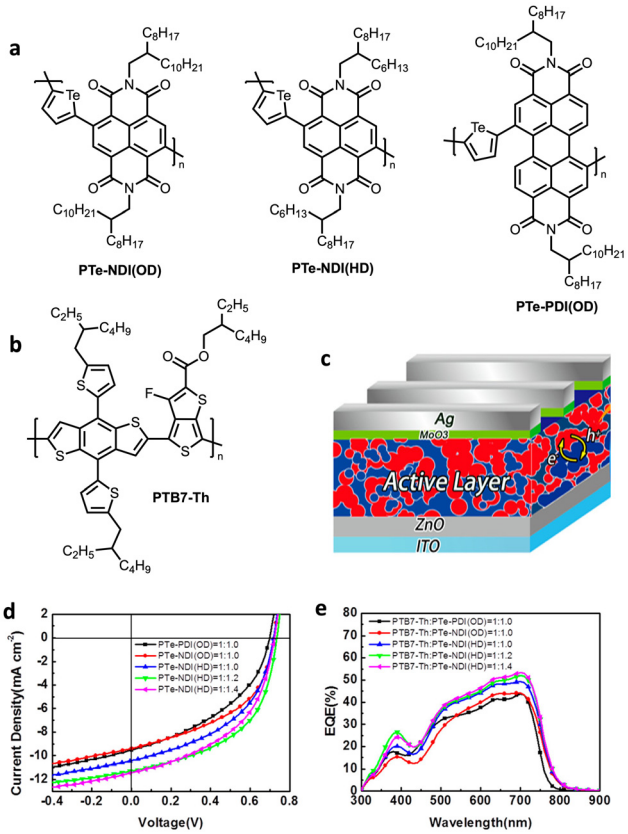

Fig. 20 Application of tellurophene polymers as n-type polymeric semiconductors and in solar cells. (a) Structures of PTe polymer donors for n-type polymeric semiconductors. OD = octyldodecyl; HD = hexyldecyl. (b) Structure of polymeric donor PTB7-Th for all-polymer solar cells. (c) Schematic of the all polymeric active layer solar cell. Blue spots represent the thiophene-based polymer donor and red spots represent the tellurophene-based polymer acceptor. (d) *J*–*V* curves and (e) external quantum efficiency (EQE) plots of organic solar cells with different active layers. Reproduced from ref. 108 with permission from American Chemical Society, copyright 2016.

4.2. Organic field-effect transistors

Conjugated semiconducting polymers have also been used in organic field-effect transistors (OFETs). These organic-based semiconductors are used in thin film form and are the active elements in OFETs that can be used as switching or logic elements in circuits.[110] Choi and coworkers examined the performance of a tellurophene-containing DPP-based D–A conjugated polymer (PDTDPPTe, **P16**) as a semiconductor in OFETs and compared it to a thiophene-containing analogue.[76] It was found that the tellurophene-based polymer showed high hole mobility, which was attributed to the better edge-on orientation of the polymer chains and strong intermolecular π–π interactions from the strong donor ability of the tellurophene.[76]

An interesting property of tellurophene that our group has reported is the ability to form coordination complexes with Br_2.[34,35] These were first reported with dihalogenated tellurophene monomers being used to prepare well-defined PTes.[34] Furthermore, these dihalogenated tellurophenes have been found to undergo thermal reductive elimination as well as photoreductive elimination to restore the Te(II) compound.[31,36] This property can be combined with thin-film transistors (TFTs) made of tellurophene-based polymers to create a sensor to detect Br_2. DPP–bitellurophene conjugated polymers were investigated for this use, and the variation of the current at fixed gate voltage allowed for the detection of Br_2 vapours.[111]

More recently, sequence-controlled conjugated polymers were examined for use in OFETs and additionally for their Br_2 detection capabilities in these transistors. Cheng and co-

workers investigated a series of sequence-controlled polymers made up of poly(3-alkylthiophene) as well as its selenophene and tellurophene analogues in alternating block copolymers (Fig. 21a).[83] These polymer arrangements were engineered to induce microphase separation between the donor and acceptor blocks. The tellurophene units undergo bromine addition (as modelled by the monomer $STePh_2$, Fig. 21b) which results in a dramatically red-shifted absorption from the alternating arrangement to induce strong charge-transfer character (Fig. 21c). Furthermore, an increase in the source–drain hole current (I_{SD}) was reported since the oxidised $PSTeBr_2$ species acts as a p-dopant on these OFETs (Fig. 21d). The reusability of these materials was demonstrated with a thermal reduction at 150 °C, which eliminates the halogens and returns the I_{SD} of the device to the neutral state (Fig. 21e).

4.3. Organic mixed ionic-electronic conductors

Another class of electroactive materials, organic mixed ionic-electronic conductors (OMIECs), have emerged recently that could be used in bioelectronic, optoelectronic, and energy storage devices.[112] These OMIECs are often polymeric semiconductors that readily solvate and transport ionic species, coupling ionic and electronic conductivity.[112] A prominent feature of these materials is the near-universal inclusion of conjugated heterocycles. The incorporation of heavier chalcogen atoms has often been employed in OPVs as a method of tuning the properties, specifically relating to optimising the HOMO–LUMOs gaps and the planarity and interactions of the backbone.[52]

Rivnay, McCulloch and coworkers synthesised a series of alternating copolymers with an oligoethylene glycol substi-

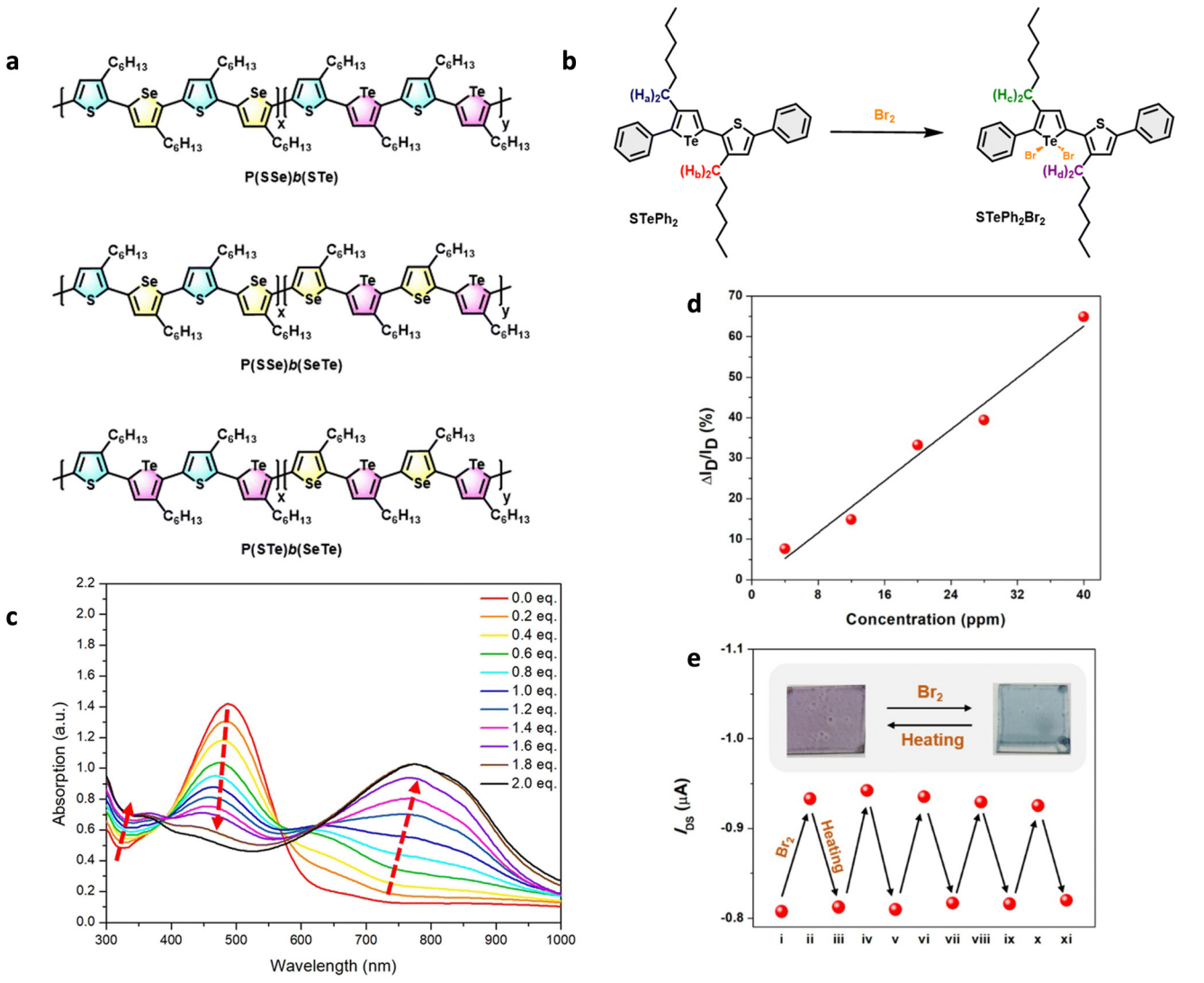

Fig. 21 Tellurophene-based polymers in OFETs. (a) Structures of alternating block copolymers **P(SSe)*b*(STe)**, **P(SSe)*b*(SeTe)** and **P(STe)*b*(SeTe)**. (b) Bromine addition to model compound monomer $STePh_2$. (c) Absorption spectra of **P(SSe)*b*(SeTe)** upon bromine titration in *o*-dichlorobenzene solution. (d) $\Delta I_{SD}/I_{SD}$ (I_{SD} = source–drain hole current) of the PSTe-based OFET device as a function of Br_2 vapor concentration. (e) I_{DS} variation of the PSTe-OFET device with V_{GS} and V_{DS} at −80 V during five cycles of Br_2 exposure followed by thermal annealing at 150 °C for 10 min. Reproduced from ref. 111 with permission from Royal Society of Chemistry, copyright 2014.

tuted bithiophenes and unsubstituted chalcogenophenes (p(g3T2-X)) where X = O, S, Se, or Te (Fig. 22a).[79] Mixed conducting properties were studied in an organic electrochemical transistor (OECT) testbeds. The doping state of p(g3T2-X) thin films in contact with aqueous electrolytes was controlled electrochemically, and the resulting electronic transport behaviour was measured. The tellurophene-containing polymer, (p(g3T2-Te)) (**P18**) showed the most ordered crystallinity, forming well-oriented edge-on 3D crystallites (Fig. 22b) in comparison to the other chalcogenophenes series, which formed 2D face-on (O), 2D mixed (S), or 2D edge-on (Se) orientations. These observations were substantiated by Grazing-Incidence Wide-Angle X-ray Scattering (GIWAXS) measurements of spin-coated thin films of the polymers. This observed crystallinity results in the (p(g3T2-Te)) polymer displaying efficient electronic charge transport, with excellent carrier mobility and volumetric capacitance. Ionic transport was found to be affected by the heteroatom-induced crystallite orientation, with edge-on oriented 2D crystallites in p(g3T2-Se) inhibiting ionic charge transport to the highest degree. (p(g3T2-Te)) was the least stable polymer under electrochemical cycling, but *in situ* GIWAXS measurements indicated that this instability was not due to structural degradation. The authors noted that instability can be overcome by recently reported modification methods.[113,114] Future studies are required on this emerging class of electroactive materials to build on the promising results seen from this study.[79]

4.4. Organic photodetectors

Organic photodetectors (OPDs) are an attractive emerging technology owing to their tunable spectral response (absorbances and wavelengths modulated by the polymer properties), light-weight nature, mechanical flexibility, and solution processability.[115,116] Tellurophene-containing polymers are particularly attractive for near-IR photo-detectors (NIR-PDs) as conventional materials such as Indium Gallium Arsenide contain scarce and toxic elements. Huang, Peng, Shen and co-workers reported tellurophene-based random copolymers with NDI and PDI for OPDs (Fig. 23a),[116] similar to those discussed for all polymer solar cells by the same group.[108] Photodetectors with a device configuration of SiO_2/ZnO/polymer/Au were fabricated (Fig. 23b). Tuning of the ratio of the electron-deficient units in the polymers allowed systematic modulation to the energy levels, light absorption and film morphology which resulted in high responsivity and excellent detectivity in the OPDs. With an optimised ratio of PDI/NDI units of 70/30 high responsivity of 19.1 A W^{-1} at 600 nm and pronounced detectivity of greater than 10^{12} Jones ranging from 350–600 nm were achieved. These high values for the OPDs were accredited to the morphology of the film, studied by AFM, which revealed the smoothest surface, endowing it with the best contact with the electrode, and lowest dark current density.

Several follow up studies were reported by the same group,[117–119] incorporating tellurophene building blocks in polymers for various OPD applications. Towards short-wave infrared (SWIR) OPDs they first reported the preparation of two polymers because of their ultranarrow band gaps; a tellurophene containing polymer, poly(benzobisthiadiazolebithiophene-tellurophene) (PBTT) and poly(benzobisthiadiazolebithiophene-4,4′-dioctyloxy-[2,2′bithiophene]) (PBTB) polymer

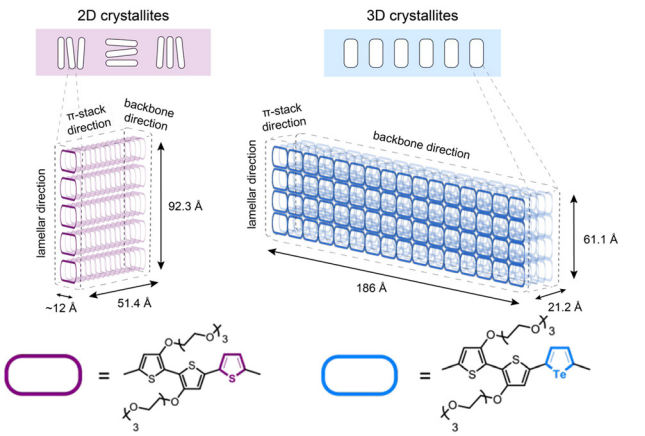

Fig. 22 Schematic graphics of the orientation of (a) p(g3T2-S) and (b) p(g3T2-Te) crystallites within the OECT channels as well as dimensionality and coherence lengths of (c) the p(g3T2-S) 2-D crystallites and (d) the p(g3T2-Te) well-oriented 3D crystallites. Reproduced from ref. 79 with permission from American Chemical Society, copyright 2024.

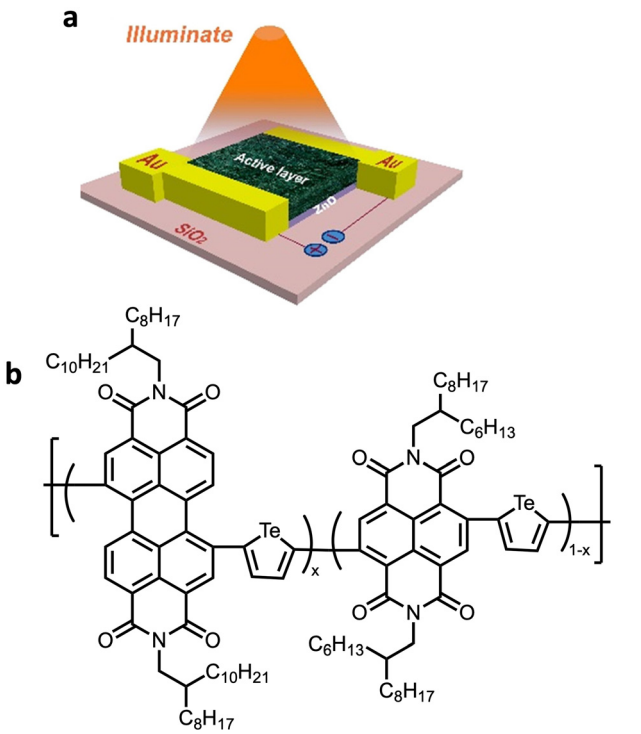

Fig. 23 Application of tellurophene-containing polymer in an OPD. (a) Device architecture for the photodetectors with SiO_2/ZnO/polymer/Au configuration. (b) Structure of random copolymers of PDI/NDI with tellurophene. Reproduced from ref. 116 with permission from American Chemical Society, copyright 2018.

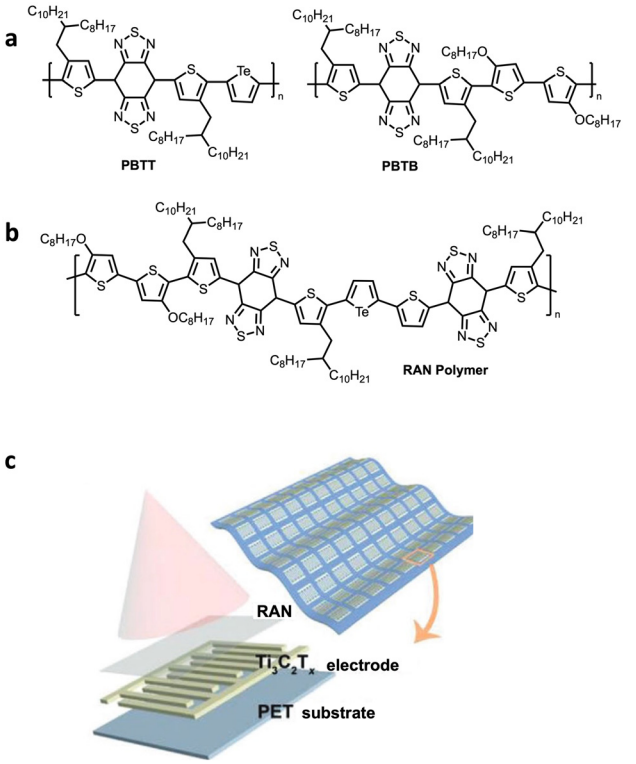

Fig. 24 Reports of telluophene-based polymers in OPD applications. (a) Polymeric structures of PBTT and PBTB used in short-wave infrared (SWIR) OPDs. (b) Structure of RAN polymer used in the NIR $Ti_3C_2T_x$-RAN PD. (c) Schematic diagram of single $Ti_3C_2T_x$-RAN PD structure. Reproduced from ref. 119 with permission from John Wiley and Sons, copyright 2022.

(Fig. 24a). Although, PBTT exhibited excellent photoresponsivity in the visible and IR regions, PBTB performed better as a PD. This was attributed to the longer lifetime of excitons, more favourable morphology (smoother film surface), and a more favourable molecular orientation relative to the substrate which facilitated better charge transport. Although not used for integration in the flexible OPD in this study, PBTT was implemented in the construction of a self-powered flexible artificial synapse for SWIR light detection, owing to the high dielectric constant and narrow band gap which contributed to spontaneous exciton dissociation.[118]

A most recent report on OPDs incorporated tellurophene as an organic photosensitive material by a Stille coupling random copolymerisation with benzo[1,2-c;4,5c′]bis[1,2,5]-thiadiazole (BBT) and bithiophene (Fig. 24b).[119] The polymer had a highly planar structure and possessed strong intramolecular charge transfer absorbance in the short-wave infrared region. The film was incorporated as a near infrared (NIR) PD array with a 2D $Ti_2C_2T_x$, an organic–inorganic heterojunction connected by van der Waals forces and hydrogen bonds (Fig. 24c). This device provides a higher on–off ratio than the Au electrode-type PD devices described above. The PDs also exhibit excellent flexibility and cycle stability.

4.5. Organic thermoelectrics

Organic thermoelectrics (OTEs) generate conductivity on application of temperature, a phenomenon known as the Seebeck effect.[120,121] Organic semiconducting polymers have garnered interest in OTEs owing to their solution processibility, lightweight, flexible nature, and low thermal conductivities.[54] However, these materials suffer from intrinsically low electronic conductivities. Methods to improve conductivity have been explored[122] including the polymerisation method,[123] modifying the degree of polymerisation,[124,125] tuning of the backbone or substituent,[126–129] doping of the polymer,[130,131] or modifying the heteroatoms in the polymer backbone.[54] Our group have investigated the optimisation of thermoelectric properties of poly(3-alkylchalcogenophene)s, P3AEs, (A = 3,7-dimethyloctyl, E = thiophene (T), selenophene (Se) or tellurophene (Te), Fig. 25a).[52,54,132] We first studied the influence of heteroatom substitutions from S to Se to Te, and the variation of $FeCl_3$ dopant concentration.[54] Moving to Te the optical band gap is narrowed, and the energy states move closer to the chemical potential, causing a decreased thermopower and increased electrical conductivity. This resulted in the highest power factor for P3ATe at lowest dopant concentration.

We further probed the structure–property relationship between P3AEs, the integration of dopants to the polymer structure.[52] P3ATe conductivity was also improved at low dopant concentration regardless of dopant selection ($FeCl_3$ or iron(III) *p*-toluenesulfonate hexahydrate). Conductivity slightly decreased at higher dopant concentrations, in contrast to the S and Se derivatives (Fig. 25b). A shift in the wide-angle X-ray diffraction (XRD) peaks also revealed heavier heteroatoms undergo structural changes to accommodate the dopant by increasing spacing between parallel chains, whereas spacing in smaller P3AT was sufficient for doping. The size of dopant anion also affected the morphology of the P3AE films in agreement with the structural changes observed in XRD. Our recent report focused on mechanism of doping.[132] P3AEs doped with 2,3,5,6-tetrafluoro-7,7,8,8-tetracyanoquinodimethane (F4TCNQ) were investigated and optical spectroscopy indicated that the quantity of dopant anion was equivalent, but that doping mechanisms varied between heteroatoms. P3AT and P3ASe were doped *via* a charge transfer complex (CTC) mechanism and P3ATe was doped through an integer charge transfer (ICT) mechanism. These mechanistic differences can be correlated to microstructure, probed by GIWAXs measurements. For P3RT and P3RSe, F4TCNQ intercalates between the π-stacked backbones resulting in CTC doping. In the P3RTe microstructure F4TCNQ intercalates in the alkyl side chain region, because of its planar packing which induces ICT doping. This results in higher conductivity for the P3ATe thin film, because of its ICT mechanism which promotes delocalised charge transfer.

4.6. Organic electrode materials for lithium-ion batteries

In the effort to move away from inorganic metals as electrode materials in batteries, organic, redox-active molecules are seen

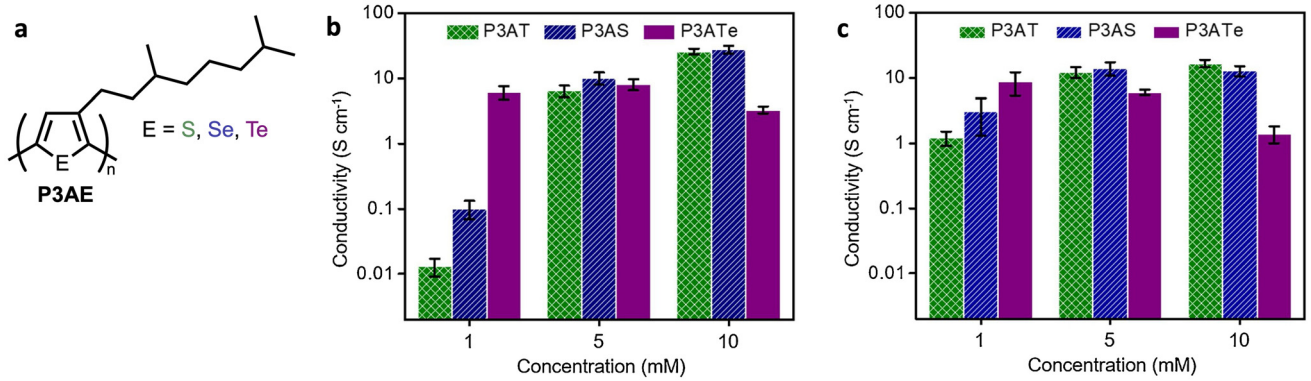

Fig. 25 Organic thermoelectric properties of poly(3-alkylchalcogenophene)s. (a) Structure of P3AEs, (A = 3,7-dimethyloctyl, E = thiophene (T), selenophene (Se) or tellurophene (Te)). Conductivity of P3AE films dip-doped at various concentrations of (b) $FeCl_3$ and (c) $FeTos_3$ solutions. Reproduced from ref. 52 with permission from Elsevier, copyright 2019.

as attractive alternatives. These organic radical batteries (ORBs) are tuneable, more sustainable, and safer than their metallic analogues.[133] The He group investigated including chalcogens into the backbone of these ORB polymer materials and found that the inclusion of these elements (S, Se, and Te) resulted in a rigid backbone, stable radical states, and extra redox centres.[85] A series of poly(chalcogenoviologen)s (Fig. 16) were synthesised, and it was found that the tellurium-based polymer derivative had a second discharge capacity and the cycle stability was enhanced dramatically.[90] The tellurium inclusion in the polymer resulted in high capacity and increased electronic conductivity in the battery material, demonstrating the capabilities of tellurium in battery electrode materials.

5. Biomedical applications of polytellurophenes and tellurophene-containing polymers

5.1. Cancer therapy

Tellurophene-containing polymers have the potential to be useful in photothermal and photodynamic cancer therapy methods. These methods are rising in popularity due to their effectiveness, non-invasive nature, and their negligible side-effects.[134,135] Photothermal therapy (PTT) uses photothermal nano-agents, which upon irradiation with a NIR laser generate heat for the thermal ablation of cancer cells.[134,136] Photodynamic therapy (PDT) involves the production of reactive oxygen species (ROS) from the irradiation of photosensitising nano-agents under NIR laser irradiation, which leads to cell death.[137] While each of these methods have their own benefits and drawbacks, their efficacy can be greatly improved if they are used in combination. PDT generates ROS to destroy cancer cells, while cell membrane permeability is increased with the mild hyperthermia that comes from PTT, promoting the uptake of these photosensitising nano-agents.[134] Tellurium nanodots have been examined in the context of PTT/PDT tumour ablation methods. These nanoparticles are capable of generating both a potent photothermal effect and ROS and is a result of the tellurium-atom in these structures, as the electrons of the tellurium nanodots are excited from the valence band to the conduction band under NIR irradiation.[138]

To gain more control over the absorption range of these agents, semiconducting polymers have emerged as a promising strategy. These polymers also show high absorption coefficients, excellent photostability, and are biocompatible.[46] The energy levels of these polymers can be altered through a D–A strategy, which is useful when trying to tune photothermal and photodynamic effects at certain wavelengths of light and achieve different functionalities in different cases.[46,135]

Huang and coworkers reported a D–A semiconducting polymer (**P21**) made using the common electron-deficient building block, naphthalene diimide (NDI), combined with bitellurophene to make PNDI-2T polymers, featuring one NDI unit and two tellurophene units per monomer.[46] Polymer nanoparticles (NPs) of ~110 nm diameter were then prepared by nanoprecipitation (Fig. 26). These materials could produce ROS, at higher quantum yields than other NPs owed in part to the increased ISC (promoted by bitellurophene). High photothermal conversion efficiencies and strong photodynamic effects for photoacoustic imaging (PAI)-guided PTT/PDT treatment were observed.

PTes have also been employed in photosensitising nano-agents in the case of hypoxic dense tumours, which have significantly lower than normal oxygen concentrations.[139] A report from the same group investigated the photothermal and photodynamic properties of copolymeric polypyrrole and PTe NPs. These NPs were prepared by oxidative copolymerisation using pyrrole and tellurophene and $FeCl_3$. Alongside the ROS, these copolymeric NPs also generated carbon-centred free radicals, which is beneficial for hypoxic PDT.[135]

5.2. Mass cytometry

One unique feature of tellurium compared to the other chalcogens is that it has eight naturally occurring isotopes, seven of

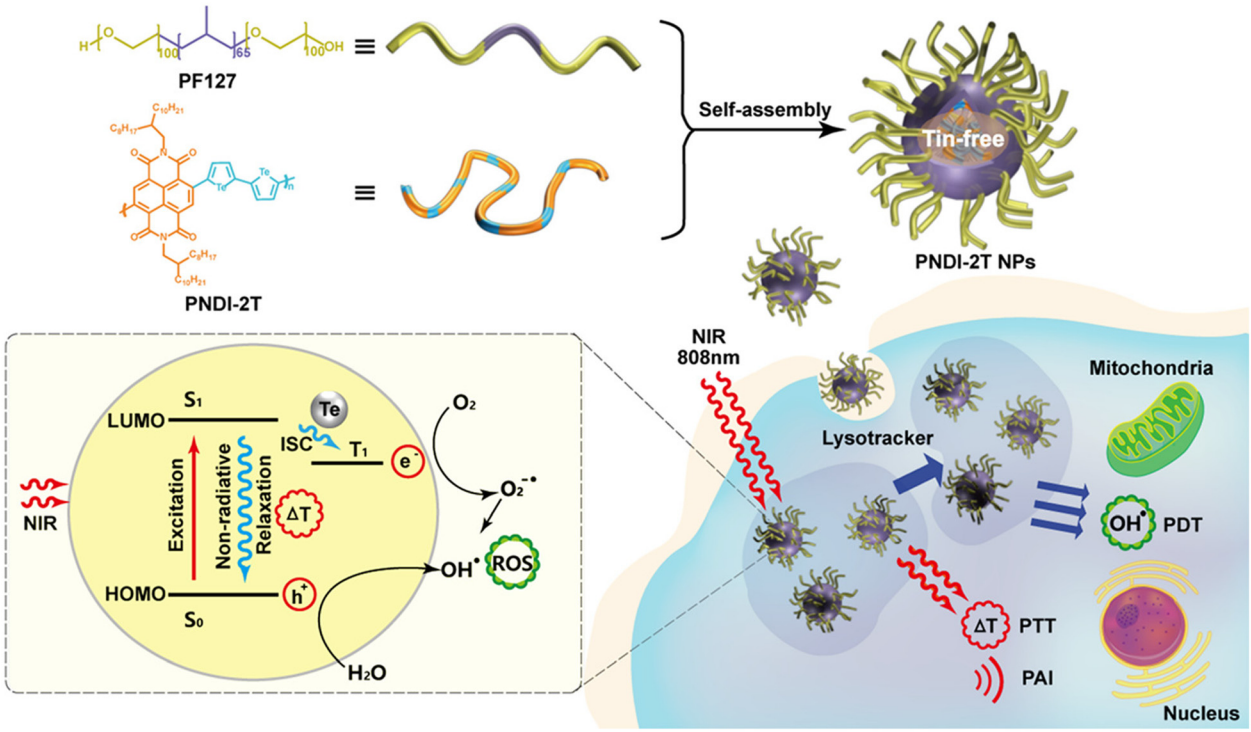

Fig. 26 Application of tellurophene-containing polymers for the generation of ROS. Schematic representation for the preparation of NPs of PNDI-2T polymer, and the proposed photophysical method for generation of ROS. Reproduced from ref. 46 with permission from American Chemical Society, copyright 2019.

which are commercially available at high levels of enrichment, making it a promising candidate for mass cytometry applications.[140] Mass cytometry is a technique used for detecting proteins and other molecules in individual cells, and it works by using metal-tagged antibodies as labels and inductively coupled plasma time-of-flight mass spectrometry (ICP-TOF-MS) as the detection method.[141] Although it is a destructive method, this technique has unique multiplexing capabilities when compared to the more conventional flow cytometry methods. The metal that the antibody is tagged with allows the examination of multiple biomarkers by monitoring signals in different mass channels.[141] Polymeric tellurophene mass tags are able to improve the sensitivity compared to small-molecule-based tellurophene probes (owing to the increased signal intensity), making them more suitable for applications in this technique.

Nitz, Winnik, and coworkers reported a water-soluble polymer with a poly-L-lysine backbone and *ca*. 48 tellurophene pendant units for mass cytometry immunoassays (Fig. 26, **P33**).[140] The study found promising results, with the polymer conjugating to primary and secondary metal-tagged antibodies (Abs). However it also revealed non-specific binding of the polymer hindered the discrimination of the positive population from the negative controls.[140] The authors noted that this may be due to interactions of the sulfate anions with positively charged cell surfaces. A second polymer with multiple polyethylene glyol (PEG) pendant group was prepared to reduce the hydrophobicity and overall negative charge (Fig. 27, **P34**). Non-specific binding was still observed, and further work is needed to optimise these tellurium-containing polymers for mass cytometry applications and to understand the binding interaction between polymer and monocytes.

5.3. Drug delivery

To date there are limited reports of tellurophene-based polymers as drug-delivery platforms/vehicles. There are, however, several reports of several tellurium-containing polymer systems for targeted drug delivery. For example, tellurium-containing polymers were studied for delivering platinum-based drugs due to tellurium's coordination chemistry with platinum.[142] This coordination enables the loading of the drug, with triggered release through competitive coordination of different biomolecules. Tellurium-based polymers are also known to be ultra-responsive to ROS.[143] Thus, they are ideal candidates to target sites of high ROS concentrations such as cancer, Alzheimer's disease, and Parkinson's disease.[144] ROS-responsive coassemblies can be fabricated from tellurium-containing polymers and phospholipids, which express a reversible change under redox conditions due to the reversible redox property of the tellurium-based molecules.[145] The ion channels formed from these coassemblies could be switched on and off by redox stimuli.[145] Tellurium-containing polymers have also been coordinated with cisplatin, which can self-assemble into nanoparticles in the aqueous phase.[146] These

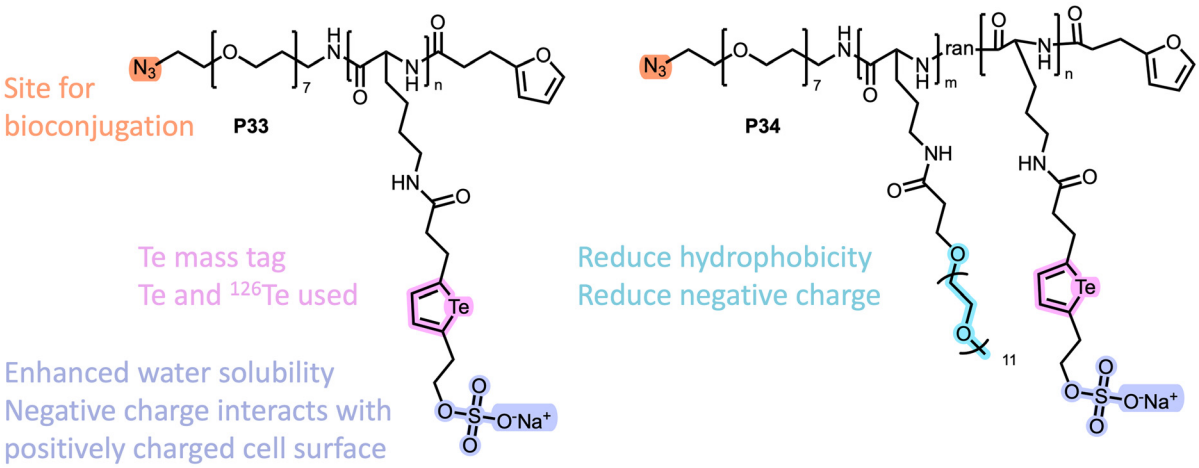

Fig. 27 Structural design of water-soluble polymers **P33** and **P34** containing tellurophene as a mass tag for application in mass cytometry, an azide group for bioconjugation and a sulfate anion to enhance water solubility. PEG pendant group added to **P34** to reduce the hydrophobicity.

nanoparticles accumulate in tumour microenvironments and kill bacteria due to the bacterial membrane disruption mechanism of tellurium.[146] Furthermore, the polymer further promote tumour cell death through ROS-induced drug delivery, which releases the complexed cisplatin inside the tumour cell.[146]

It is clear from these examples that tellurium is an interesting element in biological applications owing to its coordination chemistry, response to ROS, and multiple commercially available isotopes. In the future, incorporating tellurophene could lead to exciting advances in this field, particularly considering the development of a water-soluble tellurophene-containing polymer,[140] as well as the self-assembly capabilities of tellurophene-containing polymers,[53] which could be utilised for the formation of nanostructure motifs. Additionally, the He group has demonstrated multiple examples of using small molecule chalcogenoviologen-based materials with tellurium present for PDT,[86,88] as well as sonosensitiser for sonodynamic therapy (using ultrasound to activate and generate ROS).[89] In the future, these will likely be incorporated into polymeric structures.

6. Conclusions and outlook

In this review we have discussed the recent advances in the field of polytellurophenes (PTes) and tellurophene-containing polymers. We have discussed the inherent properties of tellurium and its five-membered heterocycle, tellurophene, and how these properties can be extended to specific targeted classes of polymers for a range of applications. We have discussed the significant progress made in the synthesis of solution-processible tellurophene monomers, that lead to solution processable polymers, which had been a major hurdle that we and others have now overcome. Despite these advances, challenges persist in synthesising homopolymers and copolymers of tellurophenes with other chalcogenophenes, such as thiophenes, which produce M_n, low $Đ$ polymers whilst also considering sustainable practices. Numerous reports that were discussed include harsh reaction conditions or toxic reagents. Developments of other chalcogenophene-polymers now include reports of high M_W, low $Đ$ polymers with few structural defects that are synthesised under mild conditions.[96]

In particular, the recent advances in numerous CTP technologies present further opportunities to prepare PTes using sustainable methods. To advance this field in the future, a focus on developing more sustainable synthetic strategies that are scalable is essential to consider any materials for industrial applications. The identification of these strategies and the discovery of new materials should be accelerated by the integration of ML[147] and AI tools for determining novel polymerisation routes and polymeric structures with enhanced understanding of structure–property relationships.[148–150] For example the emerging "polymer informatics" field, leveraging polymer research, ML and data science, should greatly accelerate the search for new polymers.[147] An issue affecting the advancement of this field in general is the ability to represent polymeric structures for data capture and search. Once these have been addressed, the ability to mine the literature for suitable reaction conditions should aid the synthetic directions for this small field of PTes. Complementary to these methods are the development of automated synthesis platforms for polymers,[151–155] which will also aid with rapid high-throughput synthesis and purification of PTes, following ML and AI guided strategies.

We briefly discussed the potential to modify substituted tellurophene monomers (*e.g.* 3-hydroxymethyltellurophene) which can offer potential access to further 3-substituted tellurophenes, reducing the number of synthetic steps. Further research into post-synthetic modification routes of monomers and indeed tellurophene-based polymers is a potential route to reduce synthetic complexity, and gain access to more synthetically challenging materials.

In the field of optoelectronics, PTes have been integrated across numerous devices including OPVs, OFETs, OMIECs and

OPDs, and significant progress has been made in the field since we last reviewed the state of the art of the field for these materials.[21,22] Of particular interest for these devices is the end of life consideration. The degradability of these materials is important,[156] and little to no information is currently known for these materials. Further exploration into the degradation and recyclability of these materials is an essential avenue for future research before consideration of potential commercialisation, a topic not unique to tellurophene-based polymers, but also the wider polymer community. This could potentially be achieved by including stimuli-responsive degradable behaviour to facilitate controlled decomposition at the end of life.[157]

Owing to the unique coordination chemistry of tellurium, its response to reactive oxygen species (ROS), and the multiple commercially available isotopes of tellurium, multiple exciting avenues for next-generation materials are available for exploration in diverse applications. Efforts to explore the self-assembly and develop biocompatible syntheses (*e.g.* by making efforts to produce water-soluble materials) will aid in this effort. Promising applications of tellurophene-containing polymers have been demonstrated in the biomedical field. This area is nascent, however, and offers opportunity for further investigations. Inspiration can be taken from examples already published for tellurium polymers, small molecules and modified tellurophenes.[86,88,89,142,143]

Focusing efforts on their greener synthesis and safe scalability will allow for exciting potential industrial applications, enabling the future capabilities of PTes materials in a sustainable and environmentally conscious world.

Conflicts of interest

There are no conflicts to declare.

Data availability

No primary research results, software or code have been included and no new data were generated or analysed as part of this review.

Acknowledgements

We gratefully acknowledge support from the NSERC of Canada (RGPIN-2022-04319).

References

1 A. H. Malik, F. Habib, M. J. Qazi, M. A. Ganayee, Z. Ahmad and M. A. Yatoo, *J. Polym. Res.*, 2023, **30**, 115.
2 K. Müllen and U. Scherf, *Macromol. Chem. Phys.*, 2023, **224**, 2200337.
3 Z. Qiu, B. A. G. Hammer and K. Müllen, *Prog. Polym. Sci.*, 2020, **100**, 101179.
4 G.-Y. Ge, J. Xu, X. Wang, W. Sun, M. Yang, Z. Mei, X.-Y. Deng, P. Li, X. Pan, J.-T. Li, X.-Q. Wang, Z. Zhang, S. Lv, X. Dai and T. Lei, *Nat. Commun.*, 2025, **16**, 396.
5 I. Song, W.-J. Lee, Z. Ke, L. You, K. Chen, S. Naskar, P. Mehra and J. Mei, *Nat. Electron.*, 2024, **7**, 1158–1169.
6 M. Ni, Z. Zhuo, B. Liu, X. Han, J. Yang, L. Sun, Y. Yang, J. Cai, X. An, L. Bai, M. Xu, J. Lin, Q. Feng, G. Xie, Y. Wu and W. Huang, *Nat. Commun.*, 2025, **16**, 330.
7 S. Wang, L. Wang, S. Ren, W. Li, Z. Wang, Z. Yi and Y. Liu, *Adv. Mater. Technol.*, 2024, **10**, 2300816.
8 Nobel Prize in Chemistry 2000, **https://www.nobelprize.org/prizes/chemistry/2000/summary/**, (accessed 4 April 2025).
9 Z. Genene, Z. Xia, G. Yang, W. Mammo and E. Wang, *Adv. Mater. Technol.*, 2024, **9**, 2300167.
10 L. Giraud, S. Grelier, E. Grau, G. Hadziioannou, C. Brochon, H. Cramail and E. Cloutet, *J. Mater. Chem. C*, 2020, **8**, 9792–9810.
11 T. Kotnik and S. Kovačič, *Eur. J. Org. Chem.*, 2025, e202400874.
12 S. C. Rasmussen, S. J. Gilman and W. D. Wilcox, *Conjugated Polymers: Synthesis & Design*, American Chemical Society, 2023. DOI: **10.1021/acsinfocus.7e7026**.
13 K. Nakabayashi, *Polym. J.*, 2018, **50**, 475–483.
14 E. F. Woods, A. J. Berl and J. A. Kalow, *ChemPhotoChem*, 2021, **5**, 4–11.
15 Q. Yang, A. Vriza, C. A. Castro Rubio, H. Chan, Y. Wu and J. Xu, *Chem. Mater.*, 2024, **36**, 2602–2622.
16 H. Cao and P. A. Rupar, *Chem. – Eur. J.*, 2017, **23**, 14670–14675.
17 T. P. Kaloni, P. K. Giesbrecht, G. Schreckenbach and M. S. Freund, *Chem. Mater.*, 2017, **29**, 10248–10283.
18 A. Patra and M. Bendikov, *J. Mater. Chem.*, 2010, **20**, 422–433.
19 A. V. Marsh and M. Heeney, *Polym. J.*, 2023, **55**, 375–385.
20 S. Ye, V. Lotocki, H. Xu and D. S. Seferos, *Chem. Soc. Rev.*, 2022, **51**, 6442–6474.
21 A. A. Jahnke and D. S. Seferos, *Macromol. Rapid Commun.*, 2011, **32**, 943–951.
22 E. I. Carrera and D. S. Seferos, *Macromolecules*, 2015, **48**, 297–308.
23 L. Wang, W. Cao and H. Xu, *ChemNanoMat*, 2016, **2**, 479–488.
24 Y. Dai, J. Guan, S. Zhang, S. Pan, B. Xianyu, Z. Ge, J. Si, C. He and H. Xu, *Prog. Polym. Sci.*, 2023, **141**, 101678.
25 T. Chivers and R. S. Laitinen, *Chem. Soc. Rev.*, 2015, **44**, 1725–1739.
26 J. Ibers, *Nat. Chem.*, 2009, **1**, 508.
27 M. A. Scarpulla, B. McCandless, A. B. Phillips, Y. Yan, M. J. Heben, C. Wolden, G. Xiong, W. K. Metzger, D. Mao, D. Krasikov, I. Sankin, S. Grover, A. Munshi, W. Sampath, J. R. Sites, A. Bothwell, D. Albin, M. O. Reese, A. Romeo, M. Nardone, R. Klie, J. M. Walls, T. Fiducia, A. Abbas and S. M. Hayes, *ol. Energy Mater. Sol. Cells*, 2023, **255**, 112289.

28 J. P. Heremans, R. J. Cava and N. Samarth, *Nat. Rev. Mater.*, 2017, **2**, 17049.
29 Z. He, Y. Yang, J.-W. Liu and S.-H. Yu, *Chem. Soc. Rev.*, 2017, **46**, 2732–2753.
30 J. Shen, S. Jia, N. Shi, Q. Ge, T. Gotoh, S. Lv, Q. Liu, R. Dronskowski, S. R. Elliott, Z. Song and M. Zhu, *Science*, 2021, **374**, 1390–1394.
31 E. I. Carrera, T. M. McCormick, M. J. Kapp, A. J. Lough and D. S. Seferos, *Inorg. Chem.*, 2013, **52**, 13779–13790.
32 F. Fringuelli, G. Marino, A. Taticchi and G. Grandolini, *J. Chem. Soc., Perkin Trans. 2*, 1974, 332.
33 N. Shida, H. Nishiyama, F. Zheng, S. Ye, D. S. Seferos, I. Tomita and S. Inagi, *Commun. Chem.*, 2019, **2**, 124.
34 A. A. Jahnke, G. W. Howe and D. S. Seferos, *Angew. Chem., Int. Ed.*, 2010, **49**, 10140–10144.
35 T. M. McCormick, A. A. Jahnke, A. J. Lough and D. S. Seferos, *J. Am. Chem. Soc.*, 2012, **134**, 3542–3548.
36 E. I. Carrera and D. S. Seferos, *Dalton Trans.*, 2015, **44**, 2092–2096.
37 E. I. Carrera, A. E. Lanterna, A. J. Lough, J. C. Scaiano and D. S. Seferos, *J. Am. Chem. Soc.*, 2016, **138**, 2678–2689.
38 C. R. B. Rhoden and G. Zeni, *Org. Biomol. Chem.*, 2011, **9**, 1301–1313.
39 Y. J. Bu, S. Tijaro-Bulla, H. Cui and M. Nitz, *J. Am. Chem. Soc.*, 2024, **146**, 26161–26177.
40 J. Bassan, L. M. Willis, R. N. Vellanki, A. Nguyen, L. J. Edgar, B. G. Wouters and M. Nitz, *Proc. Natl. Acad. Sci. U. S. A.*, 2019, **116**, 8155–8160.
41 R. Rana, R. N. Vellanki, B. G. Wouters and M. Nitz, *ChemBioChem*, 2022, **23**, e202200284.
42 J. W. Campbell, M. T. Tung, R. M. Diaz-Rodriguez, K. N. Robertson, A. A. Beharry and A. Thompson, *ACS Med. Chem. Lett.*, 2021, **12**, 1925–1931.
43 J. W. Campbell, M. T. Tung, B. B. Taylor, A. A. Beharry and A. Thompson, *Org. Biomol. Chem.*, 2024, **22**, 4157–4162.
44 R. D. Pensack, Y. Song, T. M. McCormick, A. A. Jahnke, J. Hollinger, D. S. Seferos and G. D. Scholes, *J. Phys. Chem. B*, 2014, **118**, 2589–2597.
45 D. M. González, K. N. Raftopoulos, G. He, C. M. Papadakis, A. Brown, E. Rivard and P. Müller-Buschbaum, *Macromol. Rapid Commun.*, 2017, **38**, 1700065.
46 K. Wen, X. Xu, J. Chen, L. Lv, L. Wu, Y. Hu, X. Wu, G. Liu, A. Peng and H. Huang, *ACS Appl. Mater. Interfaces*, 2019, **11**, 17884–17893.
47 M. Chattopadhyaya, S. Sen, Md. M. Alam and S. Chakrabarti, *J. Chem. Phys.*, 2012, **136**, 094904.
48 A. A. Jahnke, B. Djukic, T. M. McCormick, E. Buchaca Domingo, C. Hellmann, Y. Lee and D. S. Seferos, *J. Am. Chem. Soc.*, 2013, **135**, 951–954.
49 M. Planells, B. C. Schroeder and I. McCulloch, *Macromolecules*, 2014, **47**, 5889–5894.
50 S. Ye, L. Janasz, W. Zajaczkowski, J. G. Manion, A. Mondal, T. Marszalek, D. Andrienko, K. Müllen, W. Pisula and D. S. Seferos, *Macromol. Rapid Commun.*, 2019, **40**, 1800596.
51 A. A. Jahnke, L. Yu, N. Coombs, A. D. Scaccabarozzi, A. J. Tilley, P. M. DiCarmine, A. Amassian, N. Stingelin and D. S. Seferos, *J. Mater. Chem. C*, 2015, **3**, 3767–3773.
52 J. R. Panchuk, A. W. Laramée, J. G. Manion, S. Ye and D. S. Seferos, *Synth. Met.*, 2019, **253**, 57–61.
53 G. E. J. Hicks, C. N. Jarrett-Wilkins, J. R. Panchuk, J. G. Manion and D. S. Seferos, *Chem. Sci.*, 2020, **11**, 6383–6392.
54 S. A. Gregory, A. K. Menon, S. Ye, D. S. Seferos, J. R. Reynolds and S. K. Yee, *Adv. Energy Mater.*, 2018, **8**, 1802419.
55 R. Sugimoto, K. Yoshino, S. Inoue and K. Tsukagoshi, *Jpn. J. Appl. Phys.*, 1985, **24**, L425–L427.
56 H. Saito, S. Ukai, S. Iwatsuki, T. Itoh and M. Kubo, *Macromolecules*, 1995, **28**, 8363–8367.
57 S. Inoue, T. Jigami, H. Nozoe, Y. Aso, F. Ogura and T. Otsubo, *Heterocycles*, 2000, **52**, 159–170.
58 P. Li, T. B. Schon and D. S. Seferos, *Angew. Chem., Int. Ed.*, 2015, **54**, 9361–9366.
59 B. T. Luppi, R. McDonald, M. J. Ferguson, L. Sang and E. Rivard, *Chem. Commun.*, 2019, **55**, 14218–14221.
60 P. Pander, R. Motyka, P. Zassowski, M. Lapkowski, A. Swist and P. Data, *J. Phys. Chem. C*, 2017, **121**, 11027–11036.
61 T. Otsubo, S. Inoue, H. Nozoe, T. Jigami and F. Ogura, *Synth. Met.*, 1995, **69**, 537–538.
62 A. Patra, Y. H. Wijsboom, G. Leitus and M. Bendikov, *Org. Lett.*, 2009, **11**, 1487–1490.
63 S. Ye, PhD thesis, University of Toronto, 2019.
64 A. Kiriy, V. Senkovskyy and M. Sommer, *Macromol. Rapid Commun.*, 2011, **32**, 1503–1517.
65 S. Ye, M. Steube, E. I. Carrera and D. S. Seferos, *Macromolecules*, 2016, **49**, 1704–1711.
66 C. A. Braun, M. J. Ferguson and E. Rivard, *Inorg. Chem.*, 2021, **60**, 2672–2679.
67 S. Ye, S. M. Foster, A. A. Pollit, S. Cheng and D. S. Seferos, *Chem. Sci.*, 2019, **10**, 2075–2080.
68 S. C. Ng, H. Ding and H. S. O. Chan, *Chem. Lett.*, 1999, **28**, 1325–1326.
69 G. He, L. Kang, W. Torres Delgado, O. Shynkaruk, M. J. Ferguson, R. McDonald and E. Rivard, *J. Am. Chem. Soc.*, 2013, **135**, 5360–5363.
70 W. Torres Delgado, C. A. Braun, M. P. Boone, O. Shynkaruk, Y. Qi, R. McDonald, M. J. Ferguson, P. Data, S. K. C. Almeida, I. De Aguiar, G. L. C. De Souza, A. Brown, G. He and E. Rivard, *ACS Appl. Mater. Interfaces*, 2018, **10**, 12124–12134.
71 G. He, W. Torres Delgado, D. J. Schatz, C. Merten, A. Mohammadpour, L. Mayr, M. J. Ferguson, R. McDonald, A. Brown, K. Shankar and E. Rivard, *Angew. Chem., Int. Ed.*, 2014, **53**, 4587–4591.
72 G. He, B. D. Wiltshire, P. Choi, A. Savin, S. Sun, A. Mohammadpour, M. J. Ferguson, R. McDonald, S. Farsinezhad, A. Brown, K. Shankar and E. Rivard, *Chem. Commun.*, 2015, **51**, 5444–5447.
73 A. K. Mahrok, E. I. Carrera, A. J. Tilley, S. Ye and D. S. Seferos, *Chem. Commun.*, 2015, **51**, 5475–5478.

74 F. Zheng, A. Tanudjaja, Z. Gao, S. Inagi and I. Tomita, *Polymer*, 2020, **204**, 122809.
75 M. Al-Hashimi, Y. Han, J. Smith, H. S. Bazzi, S. Y. A. Alqaradawi, S. E. Watkins, T. D. Anthopoulos and M. Heeney, *Chem. Sci.*, 2016, **7**, 1093–1099.
76 M. Kaur, D. S. Yang, J. Shin, T. W. Lee, K. Choi, M. J. Cho and D. H. Choi, *Chem. Commun.*, 2013, **49**, 5495–5497.
77 R. S. Ashraf, I. Meager, M. Nikolka, M. Kirkus, M. Planells, B. C. Schroeder, S. Holliday, M. Hurhangee, C. B. Nielsen, H. Sirringhaus and I. McCulloch, *J. Am. Chem. Soc.*, 2015, **137**, 1314–1321.
78 E. H. Jung, S. Bae, T. W. Yoo and W. H. Jo, *Polym. Chem.*, 2014, **5**, 6545–6550.
79 B. D. Paulsen, D. Meli, M. Moser, A. Marks, J. F. Ponder, R. Wu, E. A. Schafer, J. Strzalka, Q. Zhang, I. McCulloch and J. Rivnay, *Chem. Mater.*, 2024, **36**, 1818–1830.
80 P.-F. Li, T. B. Schon and D. S. Seferos, *Angew. Chem., Int. Ed.*, 2015, **54**, 9361–9366.
81 Y. S. Park, Q. Wu, C.-Y. Nam and R. B. Grubbs, *Angew. Chem., Int. Ed.*, 2014, **53**, 10691–10695.
82 H.-H. Liu, W.-W. Liang, Y.-Y. Lai, Y.-C. Su, H.-R. Yang, K.-Y. Cheng, S.-C. Huang and Y.-J. Cheng, *Chem. Sci.*, 2020, **11**, 3836–3844.
83 K.-H. Huang, H.-H. Liu, K.-Y. Cheng, C.-L. Tsai and Y.-J. Cheng, *Chem. Sci.*, 2023, **14**, 8552–8563.
84 Y. Xue, H. Liu, K. Huang, K. Cheng, C. Tsai, C. Wu and Y. Cheng, *Chem. – Asian J.*, 2025, e202500277.
85 G. Li, L. Xu, W. Zhang, K. Zhou, Y. Ding, F. Liu, X. He and G. He, *Angew. Chem., Int. Ed.*, 2018, **57**, 4897–4901.
86 K. Zhou, R. Tian, G. Li, X. Qiu, L. Xu, M. Guo, D. Chigan, Y. Zhang, X. Chen and G. He, *Chem. – Eur. J.*, 2019, **25**, 13472–13478.
87 G. Li, R. Song, W. Ma, X. Liu, Y. Li, B. Rao and G. He, *J. Mater. Chem. A*, 2020, **8**, 12278–12284.
88 Q. Sun, Q. Su, Y. Gao, K. Zhou, W. Song, P. Quan, X. Yang, Z. Ge, Y. Zhang and G. He, *Aggregate*, 2023, **4**, e298.
89 Q. Sun, W. Song, Y. Gao, R. Ding, S. Shi, S. Han, G. Li, D. Pei, A. Li and G. He, *Biomaterials*, 2024, **304**, 122407.
90 G. Li, B. Zhang, J. Wang, H. Zhao, W. Ma, L. Xu, W. Zhang, K. Zhou, Y. Du and G. He, *Angew. Chem., Int. Ed.*, 2019, **58**, 8468–8473.
91 G. L. Gibson, T. M. McCormick and D. S. Seferos, *J. Am. Chem. Soc.*, 2012, **134**, 539–547.
92 H. Nishiyama, F. Zheng, S. Inagi, H. Fueno, K. Tanaka and I. Tomita, *Polym. Chem.*, 2020, **11**, 4693–4698.
93 F. Zheng, Y. Komatsuzaki, N. Shida, H. Nishiyama, S. Inagi and I. Tomita, *Macromol. Rapid Commun.*, 2019, **40**, 1900171.
94 F. Zheng, S.-E. Tan, Y. Yanamoto, N. Shida, H. Nishiyama, S. Inagi and I. Tomita, *NPG Asia Mater.*, 2020, **12**, 1–7.
95 M. V. Bautista, A. J. Varni, J. Ayuso-Carrillo, M. C. Carson and K. J. T. Noonan, *Polym. Chem.*, 2021, **12**, 1404–1414.
96 H. Kim, H. Yoo, H. Kim, J.-M. Park, B. H. Lee and T.-L. Choi, *J. Am. Chem. Soc.*, 2025, 11886–11895.
97 E. I. Carrera and D. S. Seferos, *Organometallics*, 2017, **36**, 2612–2621.
98 S. B. Darling and F. You, *RSC Adv.*, 2013, **3**, 17633–17648.
99 E. K. Solak and E. Irmak, *RSC Adv.*, 2023, **13**, 12244–12269.
100 L. Sun, K. Fukuda and T. Someya, *npj Flexible Electron.*, 2022, **6**, 89.
101 G. Zhang, F. R. Lin, F. Qi, T. Heumüller, A. Distler, H.-J. Egelhaaf, N. Li, P. C. Y. Chow, C. J. Brabec, A. K.-Y. Jen and H.-L. Yip, *Chem. Rev.*, 2022, **122**, 14180–14274.
102 P. G. V. Sampaio and M. O. A. González, *Int. J. Energy Res.*, 2022, **46**, 17813–17828.
103 X. Zhan and D. Zhu, *Polym. Chem.*, 2010, **1**, 409–419.
104 P. C. Srivastava, S. Bajpai, S. Bajpai, C. Ram, R. Kumar, J. P. Jasinski and R. J. Butcher, *J. Organomet. Chem.*, 2004, **689**, 194–202.
105 M. A. Baldo, D. F. O'Brien, Y. You, A. Shoustikov, S. Sibley, M. E. Thompson and S. R. Forrest, *Nature*, 1998, **395**, 151–154.
106 Y. Shao and Y. Yang, *Adv. Mater.*, 2005, **17**, 2841–2844.
107 P. Cheng and Y. Yang, *Acc. Chem. Res.*, 2020, **53**, 1218–1228.
108 L. Lv, X. Wang, X. Wang, L. Yang, T. Dong, Z. Yang and H. Huang, *ACS Appl. Mater. Interfaces*, 2016, **8**, 34620–34629.
109 L. M. Kozycz, D. Gao, A. J. Tilley and D. S. Seferos, *J. Polym. Sci., Part A: Polym. Chem.*, 2014, **52**, 3337–3345.
110 H. E. Katz and Z. Bao, *J. Phys. Chem. B*, 2000, **104**, 671–678.
111 M. Kaur, D. H. Lee, D. S. Yang, H. A. Um, M. J. Cho, J. S. Kang and D. H. Choi, *Chem. Commun.*, 2014, **50**, 14394–14396.
112 B. D. Paulsen, K. Tybrandt, E. Stavrinidou and J. Rivnay, *Nat. Mater.*, 2020, **19**, 13–26.
113 E. A. Schafer, R. Wu, D. Meli, J. Tropp, M. Moser, I. McCulloch, B. D. Paulsen and J. Rivnay, *ACS Appl. Electron. Mater.*, 2022, **4**, 1391–1404.
114 S. Zhang, P. Ding, T.-P. Ruoko, R. Wu, M.-A. Stoeckel, M. Massetti, T. Liu, M. Vagin, D. Meli, R. Kroon, J. Rivnay and S. Fabiano, *Adv. Funct. Mater.*, 2023, **33**, 2302249.
115 B. Jiang, D. Lin, M. Shiu, Y. Su, T. Tsai, P. Tsai, T. Shieh, C. K. Chan, J. Lu and C. Chen, *Adv. Opt. Mater.*, 2023, **11**, 2203129.
116 K. Zhang, L. Lv, X. Wang, Y. Mi, R. Chai, X. Liu, G. Shen, A. Peng and H. Huang, *ACS Appl. Mater. Interfaces*, 2018, **10**, 1917–1924.
117 L. Lv, W. Dang, X. Wu, H. Chen, T. Wang, L. Qin, Z. Wei, K. Zhang, G. Shen and H. Huang, *Macromolecules*, 2020, **53**, 10636–10643.
118 H. Chen, L. Lv, Y. Wei, T. Liu, S. Wang, Q. Shi and H. Huang, *Cell Rep. Phys. Sci.*, 2021, **2**, 100507.
119 C. Hu, H. Chen, L. Li, H. Huang and G. Shen, *Adv. Mater. Technol.*, 2022, **7**, 2101639.
120 M. Lindorf, K. A. Mazzio, J. Pflaum, K. Nielsch, W. Brütting and M. Albrecht, *J. Mater. Chem. A*, 2020, **8**, 7495–7507.
121 B. Russ, A. Glaudell, J. J. Urban, M. L. Chabinyc and R. A. Segalman, *Nat. Rev. Mater.*, 2016, **1**, 16050.

122 S. Wang, G. Zuo, J. Kim and H. Sirringhaus, *Prog. Polym. Sci.*, 2022, **129**, 101548.
123 I. Imae, R. Akazawa, Y. Ooyama and Y. Harima, *J. Polym. Sci.*, 2020, **58**, 3004–3008.
124 W. Shi, Z. Shuai and D. Wang, *Adv. Funct. Mater.*, 2017, **27**, 1702847.
125 S. E. Yoon, B. Kim, S. Y. Chun, S. Y. Lee, D. Jeon, M. Kim, S. Lee, B. E. Seo, K. S. Choi, F. S. Kim, T. Kim, H. Seo, K. Kwak, J. H. Kim and B. Kim, *Adv. Funct. Mater.*, 2022, **32**, 2202929.
126 J. F. Ponder, S. A. Gregory, A. Atassi, A. K. Menon, A. W. Lang, L. R. Savagian, J. R. Reynolds and S. K. Yee, *J. Am. Chem. Soc.*, 2022, **144**, 1351–1360.
127 S. H. Cho, J.-W. Ha, C. E. Song, Y. H. Kang, M. Han, S. Lee and B. Park, *J. Chem. Eng.*, 2025, **508**, 160823.
128 W. Zhu, X. Qiu, J. E. M. Laulainen, H. Un, X. Ren, M. Xiao, G. Freychet, P. Vacek, D. Tjhe, Q. He, W. Wood, Z. Wang, Y. Zhang, Z. Qu, J. Asatryan, J. Martin, M. Heeney, C. R. McNeill, P. A. Midgley, I. E. Jacobs and H. Sirringhaus, *Adv. Mater.*, 2024, **36**, 2310480.
129 J. Wu, X. Yin, F. Yang, S. Wang, Y. Liu, X. Mao, X. Nie, S. Yang, C. Gao and L. Wang, *J. Chem. Eng.*, 2022, **429**, 132354.
130 S. E. Yoon, Y. Kang, J. Im, J. Lee, S. Y. Lee, J. Park, Y. J. Gao, D. Jeon, J. Y. Son, J. Kim, C. J. Kousseff, T. Kim, H. Seo, K. Kang, I. McCulloch, S. K. Kwak, H. H. Choi, B.-G. Kim and J. H. Kim, *Joule*, 2023, **7**, 2291–2317.
131 S. Wang, W. Zhu, I. E. Jacobs, W. A. Wood, Z. Wang, S. Manikandan, J. W. Andreasen, H. Un, S. Ursel, S. Peralta, S. Guan, J. Grivel, S. Longuemart and H. Sirringhaus, *Adv. Mater.*, 2024, **36**, 2314062.
132 M. P. Gordon, S. A. Gregory, J. P. Wooding, S. Ye, G. M. Su, D. S. Seferos, M. D. Losego, J. J. Urban, S. K. Yee and A. K. Menon, *Appl. Phys. Lett.*, 2021, **118**, 233301.
133 Y. Imada, H. Nakano, K. Furukawa, R. Kishi, M. Nakano, H. Maruyama, M. Nakamoto, A. Sekiguchi, M. Ogawa, T. Ohta and Y. Yamamoto, *J. Am. Chem. Soc.*, 2016, **138**, 479–482.
134 W. Fan, B. Yung, P. Huang and X. Chen, *Chem. Rev.*, 2017, **117**, 13566–13638.
135 K. Wen, L. Wu, X. Wu, Y. Lu, T. Duan, H. Ma, A. Peng, Q. Shi and H. Huang, *Angew. Chem., Int. Ed.*, 2020, **59**, 12756–12761.
136 J. Yu, D. Javier, M. A. Yaseen, N. Nitin, R. Richards-Kortum, B. Anvari and M. S. Wong, *J. Am. Chem. Soc.*, 2010, **132**, 1929–1938.
137 Q. Wang, Y. Dai, J. Xu, J. Cai, X. Niu, L. Zhang, R. Chen, Q. Shen, W. Huang and Q. Fan, *Adv. Funct. Mater.*, 2019, **29**, 1901480.
138 T. Yang, H. Ke, Q. Wang, Y. Tang, Y. Deng, H. Yang, X. Yang, P. Yang, D. Ling, C. Chen, Y. Zhao, H. Wu and H. Chen, *ACS Nano*, 2017, **11**, 10012–10024.
139 Z. Chen, F. Han, Y. Du, H. Shi and W. Zhou, *Signal Transduction Targeted Ther.*, 2023, **8**, 70.
140 Y. Zhang, R. Rana, P. Liu, N. Zabinyakov, M. Nitz and M. A. Winnik, *Eur. Polym. J.*, 2022, **181**, 111633.
141 D. R. Bandura, V. I. Baranov, O. I. Ornatsky, A. Antonov, R. Kinach, X. Lou, S. Pavlov, S. Vorobiev, J. E. Dick and S. D. Tanner, *Anal. Chem.*, 2009, **81**, 6813–6822.
142 W. Cao, Y. Gu, M. Meineck, T. Li and H. Xu, *J. Am. Chem. Soc.*, 2014, **136**, 5132–5137.
143 W. Cao, Y. Gu, T. Li and H. Xu, *Chem. Commun.*, 2015, **51**, 7069–7071.
144 A. A. Alfadda and R. M. Sallam, *BioMed Res. Int.*, 2012, **2012**, 936486.
145 L. Wang, F. Fan, W. Cao and H. Xu, *ACS Appl. Mater. Interfaces*, 2015, **7**, 16054–16060.
146 J. Hu, S. Ran, Z. Huang, Y. Liu, H. Hu, Y. Zhou, X. Ding, J. Yin and Y. Zhang, *Acta Biomater.*, 2024, **185**, 323–335.
147 W. Ge, R. De Silva, Y. Fan, S. A. Sisson and M. H. Stenzel, *Adv. Mater.*, 2025, **37**, 2413695.
148 K. M. Jablonka, G. M. Jothiappan, S. Wang, B. Smit and B. Yoo, *Nat. Commun.*, 2021, **12**, 2312.
149 A. N. Wilson, P. C. St John, D. H. Marin, C. B. Hoyt, E. G. Rognerud, M. R. Nimlos, R. M. Cywar, N. A. Rorrer, K. M. Shebek, L. J. Broadbelt, G. T. Beckham and M. F. Crowley, *Macromolecules*, 2023, **56**, 8547–8557.
150 S. Nanjo, Arifin, H. Maeda, Y. Hayashi, K. Hatakeyama-Sato, R. Himeno, T. Hayakawa and R. Yoshida, *npj Comput. Mater.*, 2025, **11**, 1–11.
151 M. Rubens, J. Van Herck and T. Junkers, *ACS Macro Lett.*, 2019, **8**, 1437–1441.
152 S. T. Knox, S. J. Parkinson, C. Y. P. Wilding, R. A. Bourne and N. J. Warren, *Polym. Chem.*, 2022, **13**, 1576–1585.
153 V. F. Jafari, Z. Mossayebi, S. Allison-Logan, S. Shabani and G. G. Qiao, *Chem. – Eur. J.*, 2023, **29**, e202301767.
154 A. Vriza, H. Chan and J. Xu, *Chem. Mater.*, 2023, **35**, 3046–3056.
155 G. Tom, S. P. Schmid, S. G. Baird, Y. Cao, K. Darvish, H. Hao, S. Lo, S. Pablo-García, E. M. Rajaonson, M. Skreta, N. Yoshikawa, S. Corapi, G. D. Akkoc, F. Strieth-Kalthoff, M. Seifrid and A. Aspuru-Guzik, *Chem. Rev.*, 2024, **124**, 9633–9732.
156 A. Uva, S. Michailovich, N. S. Y. Hsu and H. Tran, *J. Am. Chem. Soc.*, 2024, **146**, 12271–12287.
157 B. R. Varju, A. J. Lough and D. S. Seferos, *Macromolecules*, 2025, **58**, 1214–1222.

